Microbiota/gut/neuron axis promotes *Drosophila* ageing via *Acetobacter, Tachykinin,* and *TkR99D*

Diana Marcu[1], David R Sannino[1], Anthony J Dornan[1,2], Rita Ibrahim[1], Atharv Kapoor[1], Miriam Wood[1], Adam J Dobson[1†]

1 - School of Molecular Biosciences, College of Medical Veterinary and Life Sciences, University of Glasgow, G12 8QQ, United Kingdom

2 - Cellular Analysis Facility - Shared Research Facilities, College of Medical Veterinary and Life Sciences, University of Glasgow, G12 8TA, United Kingdom

† For correspondence: adam.dobson@glasgow.ac.uk

Abstract

Gut microbiota exert an evolutionarily conserved influence on ageing, from invertebrates to humans. How do microbes that are physically confined to the gut lumen affect the systemic physiological process of ageing? In female *Drosophila*, we show that microbiota increase expression of the peptide hormone *Tachykinin (Tk)*, which corresponds to reduced lifespan. *Tk* is required for microbiota to shorten lifespan, with knockdown rendering flies constitutively long-lived even in the presence of an intact microbiota. This lifespan extension does not come with canonical costs to fecundity or feeding, but impacts on triacylglyceride (TAG) storage suggest adaptive functions in metabolic homeostasis. In flies with defined (gnotobiotic) microbiotas, we show that we can model *Tk*-dependent effects of microbiota on lifespan and TAG by monoassociation with *Acetobacter pomorum*. These effects require *Tk* in the midgut, and the cognate TK receptor *TkR99D* in neurons, implicating a microbiota-gut-neuron relay. This relay also appears to compromise gut barrier function in aged flies, indicating roles in healthspan as well as lifespan. However, the effect of *TkR99D* is independent of its reported role in insulin signalling and adipokinetic hormone signalling which, respectively, are canonical regulators of lifespan and TAG metabolism, suggesting a non-canonical role for *TkR99D* elsewhere in the nervous system. Altogether our results implicate a microbiota-gut-neuron axis in ageing, via a specific bacterium modulating activity of a specific and evolutionarily-conserved hormone.

Introduction

Gut microbiota influence lifespan and ageing across species. This effect appears to be evolutionarily conserved from the invertebrate models *Caenorhabditis elegans* and *Drosophila melanogaster* [1–7], through to vertebrates including fish and rodents [8–12]. Microbiota are also thought to play a role in human ageing [13,14], supported by mendelian randomisation analysis indicating a putatively causal role [15] (but see also [16]). The microbiota are physically confined to the gut lumen, yet they influence ageing at an organismal level. By what mechanisms do microbiota modulate these systemic processes?

Evolutionary theories of ageing lead us to expect that mechanisms of ageing should have adaptive functions early in life, i.e. processes under positive selection in early life have deleterious pleiotropic effects in later life, which manifest as ageing[17] . Microbiota conform to this expectation, with their impacts on ageing appearing to trade off against widespread benefits to host health early in life. For example, microbiota commonly promote host development time, even with the same species of bacteria demonstrated to benefit host development across different phyla of animals [18–20]. This motivates research to characterise how to decouple beneficial effects of microbiota early in life from deleterious effects in late life.

The capacity of microbiota to impact systemic processes, from a physically confined niche in the intestinal lumen, implicates endocrine signalling between organs. A role mediated by endocrine signalling is also consistent with the pleiotropic effects of microbiota, since hormones potently impact multiple traits. The relationship between microbiota and endocrine signalling may be bidirectional, with the microbiota altering how the gut - the biggest endocrine organ in animals - communicates lumen conditions to distal tissues, while distal tissues may direct how the gut manages the microbiota. Signalling in either direction has the potential to modulate ageing, with hormones serving as a key relay.

We chose to investigate these processes in the fruitfly *Drosophila melanogaster*. Flies can be reared axenic (i.e. without exogenous bacteria), and have a simple microbiota dominated by two families of bacteria (*Acetobacteraceae* and *Lactobacillaceae*). These bacteria can be cultured easily, and reintroduced to axenic fly eggs to generate gnotobiotic animals, enabling mapping of host phenotype to bacterial species. Fly genetics also enable tissue- and cell-type-specific genetic manipulations, e.g. expressing RNAi in specific locations, ideal for studying tissue-tissue signalling. We capitalised on these strengths to identify how defined bacteria modulate hormone signalling, and how ageing phenotypes are modulated by tissue-specific lesions in this signalling.

Results

A role for *Tk* in lifespan regulation by microbiota

72 First, we looked for evidence that microbiota modulate fly endocrine signalling. Hormone activity both
73 to and from the gut could be relevant to impact of microbiota, but the gut is the largest endocrine organ,
74 the site of physical contact with gut microbiota, and numbers of enteroendocrine cells (EEs) can vary
75 plastically in adults, which we reasoned could serve as a proxy for overall endocrine signalling capacity.
76 When we counted absolute numbers of EEs in whole guts (Figure 1A), we found more cells in guts of
77 conventionally-reared (CR) flies than in axenic flies, suggesting that microbiota enhance capacity for
78 endocrine signalling. Previous studies have shown that microbiota reduce the percentage of EEs [21,22],
79 which we suggest may have been driven by an even greater microbial promotion of other epithelial cell
80 populations, reducing proportion of EEs despite increased total numbers of EEs.
81
82 EEs express 14 peptide hormones. We asked whether microbiota promote expression of any of these
83 specifically, by reanalysing public transcriptome data [23] (Figure 1B). We were able to quantify
84 expression of 13 genes, and we analysed the fourteenth (*Burs*) by RT-qPCR (Figure S1). Four hormone
85 genes were differentially expressed. Of these four, Tachykinin (*Tk*) - which encodes orthologues of the
86 mammalian neuropeptides Substance P and Neurokinins A/B - appeared a particularly interesting
87 candidate, because published data indicated that *Tk* knockdown flies phenocopy the longer lifespan
88 and metabolic phenotypes observed in axenic flies [4,24–27]. Since the differential expression analysis was
89 performed on public data, we validated the impact of microbes on *Tk* expression in our lab stock
90 (*Dahomey*) by RT-qPCR (Figure 1C). This correlation between microbial promotion of *Tk* expression
91 and shortening of lifespan, coupled to phenocopying between axenic and *Tk* knockdown flies, led us to
92 predict that *Tk* knockdowns would be constitutively long-lived and their lifespan should no longer
93 respond to microbiota.
94

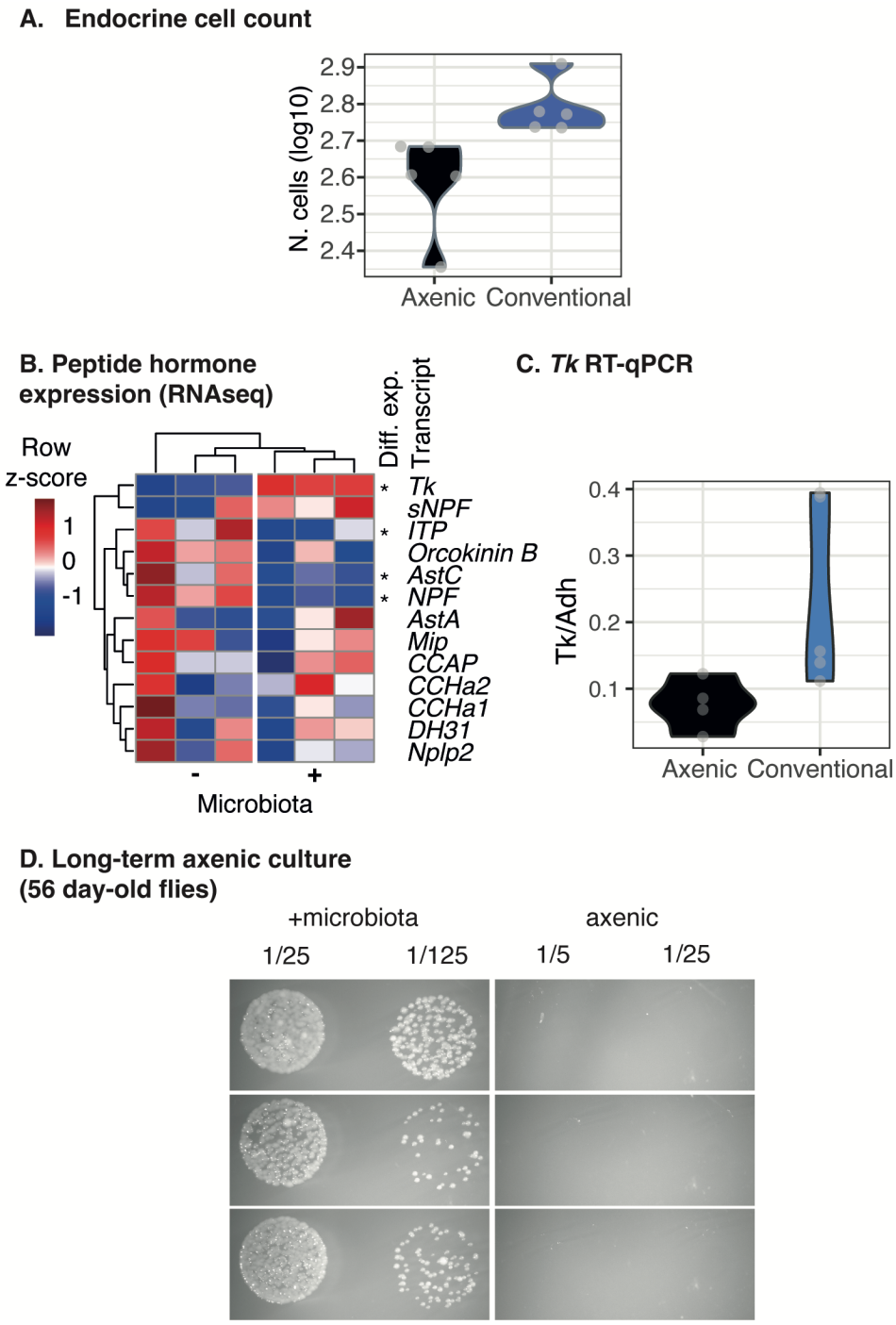

Figure 1. Basis for study: evidence that *Tk* responds to microbiota. A. Microbiota increase total number of enteroendocrine cells (EEs) in fly midgut. Number of GFP+ cells were scored in 5-day old *UAS-mCD8::GFP; Voila-Gal4* females. Wilcoxon test, W=25, P=0.008. **B.** Microbiota alter expression of peptide hormones in the *Drosophila* intestine. Transcriptome data from [23] were reanalysed. Expression of neuropeptide hormone gene transcripts are plotted, dendrograms show hierarchical clustering on Euclidian distance. Differentially expressed transcripts (DESeq2, FDR<0.1) are marked with an asterisk to right. Presence of microbiota increased expression of *Tachykinin* (top row). Software did not quantify *Burs* expression, so complementary RT-qPCR data were collected, showing no impact of microbiota (Figure S1). **C.** Confirmation that microbiota promote *Tk* expression. Expression was

quantified by RT-qPCR (using cDNA generated from midgut to complement RNA-seq data). Wilcoxon test W=1, p=0.04. **D.** Confirmation of lifelong axenic culture without antibiotics. Photographs show bacterial growth (or lack of) in homogenates of pools of 3 females, reared to day 56 of adulthood either with bacteria or axenic, serial dilutions indicated at top.

We tested our prediction by assessing impact of *Tk* knockdown in flies reared with/without a microbiota. We reared flies under axenic conditions from embryo until death, to avoid potential off-target effects on the fly of antibiotic feeding [28–30], after confirming that we could maintain sterile culture conditions throughout the lifespan (Figure 1D). To establish the genetic role of *Tk*, we first used a ubiquitous knockdown, to avoid in the first instance the possibility that targeting one specific tissue may lead to compensatory expression in another. We drove RNAi expression using an inducible ubiquitous driver (*Daughterless-GeneSwitch* a.k.a. *DaGS)*, which we activated in 3-day-old adult females by feeding a chemical inducer, RU486 (henceforth, RU), thereby avoiding any possible confounding impacts of knockdown during development. In all experiments, we used female flies and a fully-factorial design.

Microbiota shortened lifespan relative to axenic controls (Figure 2A). However, Tk^{RNAi} blocked this effect, rendering CR flies as long-lived as axenics. Cox Proportional Hazards analysis (CoxPH) revealed a significant Tk^{RNAi}:microbiota interaction (p=0.05), and post-hoc tests (Fig 2b). We also used EMMs to plot *post hoc* metrics of differences in survival, multiplied by -1 such that higher values corresponded to extended lifespan: this metric further underlined the *Tk**microbiota interaction, demonstrating a significant shortening of lifespan in controls but not with Tk^{RNAi} (Fig 2b). CR lifespan was not extended by RU in the absence of the *UAS-*Tk^{RNAi} transgene (Figure S2), indicating that the *Tk*:microbiota interaction was attributable to knockdown, not off-target effects of RU feeding. These results indicated that *Tk* was required for microbiota to modulate lifespan.

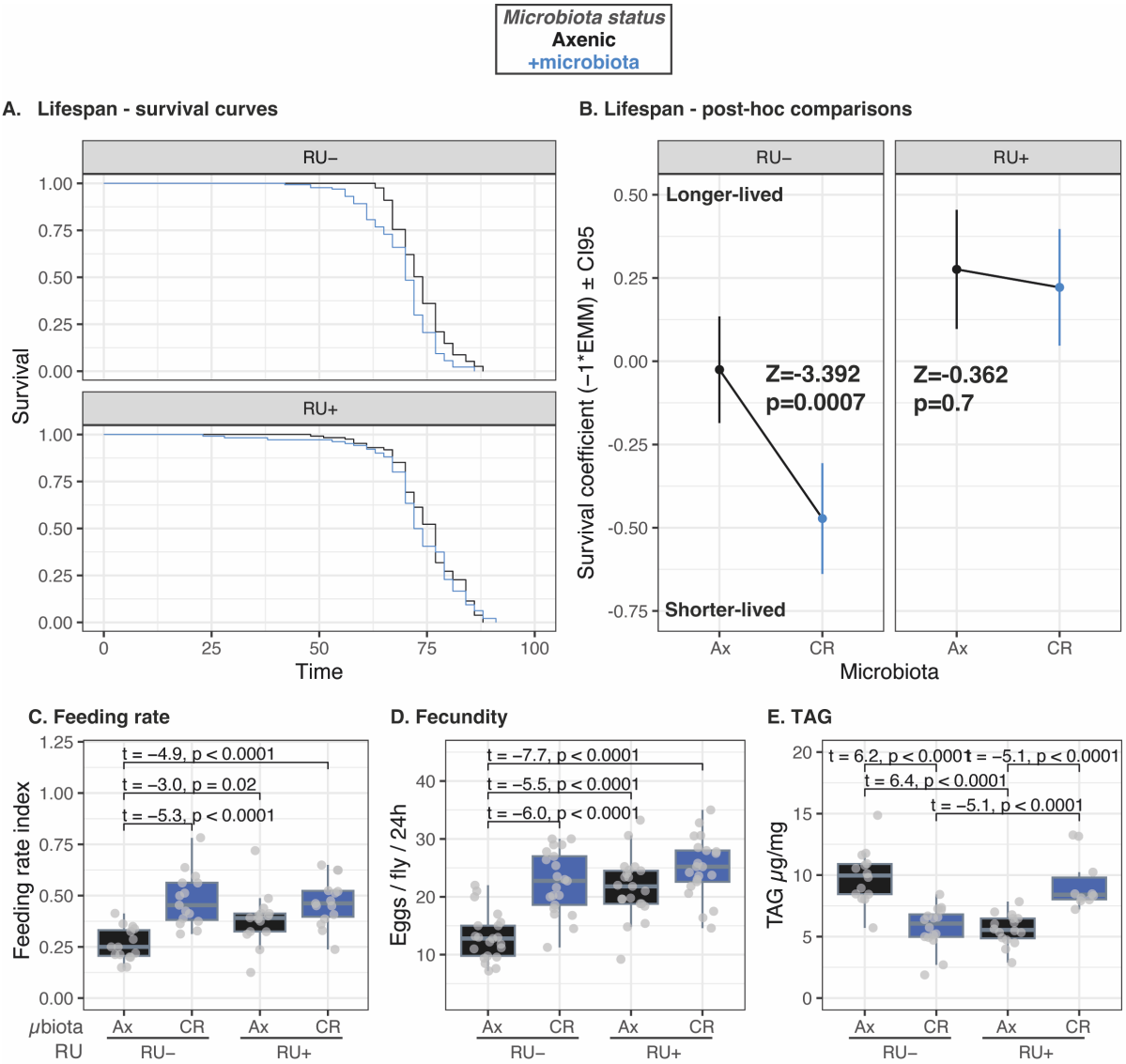

Figure 2. Ubiquitous *Tk* is required for microbiota to shorten lifespan and reduce TAG storage. **A.** Kaplan-Meier plots showing survival of axenic and conventionally-reared (CR) *DaGS;UAS-Tk*^{RNAi} flies, faceted by absence/presence (top/bottom) of transgene activation by RU486 (RU). Cox Proportional Hazards analysis revealed an RU:microbiota interaction (p=0.05). **B.** Post-hoc analysis of survival data shown in A. Facets show estimated marginal means of Cox Proportional Hazards model (EMMs±95% confidence intervals (CI95)), multiplied -1*n to make higher values correspond to longer lifespan. Pairwise tests (text on facets) revealed impact of microbiota only in absence of RU. **C-D.** *Tk*^{RNAi} (RU+) does not block effect of microbiota on feeding rate (C) or fecundity (D). Feeding quantified as average proboscis extension rate per vial (n=5 mated females/vial, 10 days old after 7 days feeding on RU/vehicle.). Fecundity quantified as n. eggs laid per fly over 24h (n=5 females/vial). **E.** *Tk*^{RNAi} (RU+) blocks reduction of TAG by microbiota. Points give TAG μg mg^{-1} in pools of five flies. The result was replicated with an independent RNAi construct (Figure S3). Panels A-E generated with RNAi construct V330743. Panels A-B, n=135-136 flies per condition. Panels C-E, Statistics on brackets are from *post-*

145 *hoc* EMM analyses of linear models (C, logit-transformed data), when significant differences were
146 detected.
147
148 **Evidence for pleiotropic roles of *Tk* between lifespan and metabolism, but not canonical**
149 **tradeoffs with ageing**
150 Tachykinins are highly pleiotropic peptides [31], and interventions that extend lifespan are commonly
151 associated with pleiotropic trade-offs early in life. For example, lifespan is expected to anticorrelate
152 reproduction in early life [32], while feeding behaviour, naturally selected to optimise growth and
153 reproduction, is expected to be deleterious for ageing [33–36]. We therefore hypothesised that Tk^{RNAi} might
154 block beneficial effects of microbiota on reproduction or feeding in early life. We measured steady-state
155 feeding behaviour (proboscis extension) and a point measure of fecundity (egg laying over 24h), after
156 one week of Tk^{RNAi} induction in both axenic and CR flies. As expected, microbiota did indeed increase
157 feeding and egg laying in CR flies relative to axenics (Fig 2C-D), but Tk^{RNAi} did not reduce either
158 fecundity or feeding. Thus, longevity in CR Tk^{RNAi} flies appears not to be associated with canonical
159 costs.
160
161 We looked for alternative pleiotropic traits. Microbiota have evolutionarily-conserved effects on host
162 metabolism, with increased lipid storage observed in axenic hosts [27,37,38]. Since *Tk* is also implicated in
163 mobilising fly triglyceride (TAG) stores [25], we anticipated a potential tradeoff with lifespan. Without
164 Tk^{RNAi}, microbiota reduced TAG storage as expected, but Tk^{RNAi} blocked this effect in two replicate
165 experiments with distinct Tk^{RNAi} constructs (Figure 2E, Figure S3). These results suggested a pleiotropic
166 role for *Tk* in managing metabolic responses to microbiota in early life, with deleterious impacts in late
167 life.
168
169 ***Acetobacter pomorum,* but not *Levilactobacillus brevis*, interacts with *Tk* to determine lifespan**
170 **and TAG**
171 Can the interaction between microbiota and *Tk* be attributed to particular gut bacteria? The fly
172 microbiota, while relatively simple, still contains numerous taxa, which vary among strains and
173 environments, but tend to contain families *Acetobacteraceae and Lactobacillaceae* [39–43]. We
174 characterised the fly microbiota in our lab background by 16S rRNA amplicon sequencing, and identified
175 amplicon sequencing variants (ASVs). Most ASVs were assigned to the family *Acetobacteraceae*
176 (Figure 3a), and *Lactobacillaceae* were also present (among other families). *Acetobacter pomorum* and
177 *Levilactobacillus brevis* are two well-studied strains that can be considered representatives of their
178 respective genera, on the basis of genome content [44] and phenotypic impacts [45] . We asked whether
179 either *A. pomorum* or *L. brevis* alone recapitulated impacts of a CR microbiota on lifespan and TAG,
180 and whether they interacted equivalently with Tk^{RNAi}.
181
182 We generated gnotobiotic flies, monoassociated with either *A. pomorum* (DmCS004) or *L. brevis*
183 (DmCS003), along with axenic controls, and tested whether lifespan impacts were blocked by

ubiquitous *Tk*^{RNAi} (Figure 3B-C). Without *Tk*^{RNAi}, axenic flies were longest-lived, flies associated with *A. pomorum* (henceforth *Ap*-flies) were shortest-lived, and flies associated with *L. brevis* (*Lb*-flies) were intermediate. However, *Tk*^{RNAi} induction rendered flies constitutively long-lived, independent of microbiota association and equivalent to axenic controls. Thus, *Tk*^{RNAi} blocked variation in lifespan caused by synthetic variation in the microbiota, and this effect was strongest in *Ap*-flies.

We quantified *Tk* expression by RT-qPCR among axenic flies, *Lb*-flies and *Ap*-flies, and asked whether change in expression upon knockdown (*DaGS, UAS-Tk*^{RNAi}) correlated lifespan outcome (Figure S4). *Tk* expression was lowest in axenics, highest in *Ap*-flies, and intermediate in *Lb*-flies (Figure S4A), but RU feeding arrested *Tk* expression across all three microbiota conditions - confirming universally efficient knockdown - and this expression level was equivalent to control axenic flies (Figure S4A). Plotting *Tk* expression against statistical coefficients (EMMs) of the corresponding survival data, revealed a correlation across conditions between *Tk* expression values and lifespan (Figure S4B). Thus, microbial modulation of lifespan appears to correspond to organismal expression of *Tk*.

We then asked whether specific bacteria and *Tk* interactively modulated TAG levels in youth (Figure 3E). We found reduced TAG in *Ap*-flies relative to axenic flies, and this effect was reversed by *Tk*^{RNAi}, consistent with the pleiotropic tradeoff we had observed in CR flies. However no interaction was apparent between *L. brevis* and *Tk*^{RNAi}. Thus, *A. pomorum* was sufficient to modulate TAG in interaction with *Tk*, but *L. brevis* was not.

Altogether, these data demonstrated that *A. pomorum* is sufficient to fully recapitulate the impacts of a complete microbiota on both lifespan and TAG, and interacts equivalently with ubiquitous *Tk*^{RNAi}. By comparison the intermediate effects in *Lb*-flies argues against *Lactobacillaceae* playing a leading role in the *Tk*-dependent regulation of lifespan and TAG.

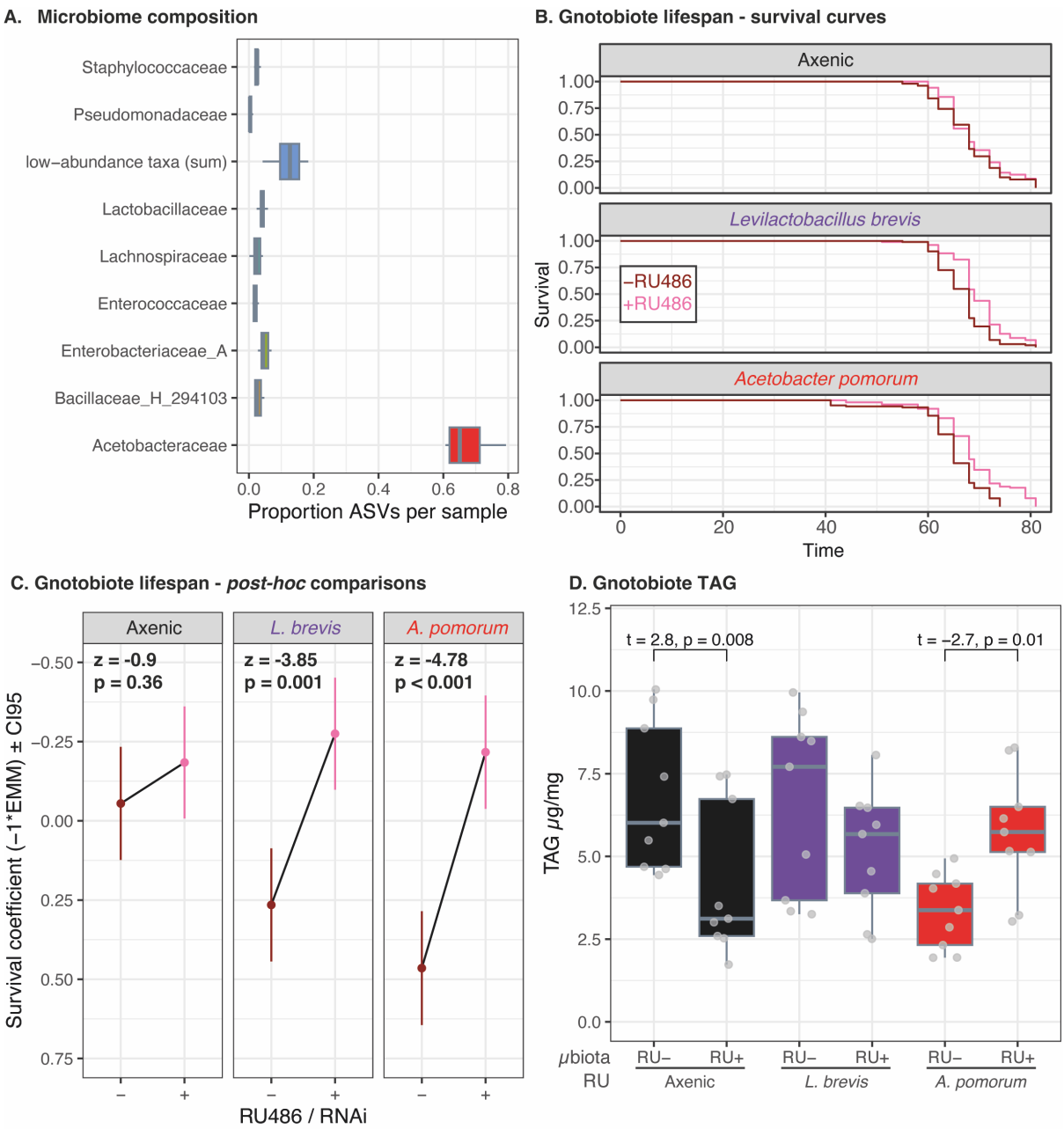

Figure 3. Phenotypic impact of a complete microbiota and interaction with ubiquitous *Tk^{RNAi}* is recapitulated fully by *Acetobacter pomorum*, but only partially by *Levilactobacillus brevis.* A. 16s rRNA amplicon sequencing reveals microbiota dominated by family *Acetobacteraceae* in the *Dahomey* fly background. Plot shows proportion ASVs per sample assigned to given families. "low abundance taxa" denotes a bin of all ASVs not assigned to one of the given families. ~170k reads per sample, n=10 samples. **B.** Kaplan-Meier plots showing survival of *DaGS;UAS-Tk^{RNAi}* flies (RNAi construct V330743), cultured either under axenic or gnotobiotic conditions. Gnotobiotic flies were cultured in monoassociation with either *Acetobacter pomorum* (*Ap*-flies) or *LeviLevilactobacillus brevis* (*Lb*-flies). Plots are faceted by microbial condition. Cox Proportional Hazards analysis revealed an RU:microbiota interaction (p=0.02). **C.** Post-hoc analysis of survival curves shown in B. Plots show a survival coefficient, calculated from estimated marginal means of Cox Proportional Hazards model (EMMs±95% confidence intervals (CI95)), multiplied -1*n such that higher values correspond to longer

222 lifespan. Pairwise tests (text on facets) revealed effect of Tk^{RNAi} induction (+RU) was largest in *Ap*-flies,
223 intermediate in *Lb*-flies, and no effect was observed in axenics. **D.** *A. pomorum,* but not *L. brevis,*
224 recapitulates effects of a complete microbiota on TAG. Points give TAG μg mg^{-1} in pools of five flies
225 (n=9). Significant interaction of microbiota and *TkRNAi* (RU) was detected (ANOVA F=6.96, df=2,48,
226 p=0.002). Statistics on brackets are from *post-hoc* EMM analyses of linear models, when significant
227 differences were detected.
228
229 ***A. pomorum* modulates *Tk* expression in midgut but not CNS.**
230 Our initial experiments employed ubiquitous Tk^{RNAi}. From which specific tissue does *Tk* knockdown
231 mediate effects of the microbiota? Plotting steady-state (microbiota-independent) *Tk* expression, using
232 FlyAtlas2 data [46], revealed that *Tk* is enriched in neuronal and midgut tissues (Figure 4A). We therefore
233 characterised metrics of Tachykinin activity from these two tissues in axenic flies, *Lb*-flies and *Ap*-flies.
234 We examined *Tk* expression by RT-qPCR of RNA from heads and on dissected midguts. *A. pomorum*
235 increased *Tk* expression in midgut, but not in heads; while *L. brevis* did not impact *Tk* expression in
236 either tissue (Figure 4B). We used reporters to confirm intestinal modulation of *Tk* expression.
237 *Acetobacter* are thought to promote Tk signalling epigenetically, by promoting histone lysine acetylation
238 in *Tk+* cells [47]. We confirmed that lysine acetylation was labile in *Tk+* EEs by feeding axenic flies with
239 a histone deacetylase inhibitor, trichostatin-A, and quantifying staining in *Tk+* cells in both anterior and
240 posterior regions of the midgut (Figure 4C-D). We then examined effects of microbiota, finding
241 increased acetyl-lysine in *Tk+* cells of *Ap*-flies, but not *Lb*-flies (Figure 4D). We asked whether this
242 increase corresponded to elevated *Tk* expression, and indeed *Tk* reporter expression (*Tk-T2A-*
243 *Gal4>UAS*-GFP) was elevated in the anterior midgut (Figure 4E). However, reporter activity was not
244 increased in posterior midgut (Figure 4E). Together, these results confirm previous observations that
245 *A. pomorum* increases lysine acetylation in *Tk+* EEs, suggesting possible epigenetic regulation or
246 priming of *Tk* regulation, but correspondence between lysine acetylation and *Tk* reporter expression
247 appears specific to certain regions of the midgut.
248
249 Having shown that *Tk* expression was activated specifically by *A. pomorum* in the midgut, but not by *L.*
250 *brevis*, we focussed specifically on *A. pomorum* in subsequent experiments.
251

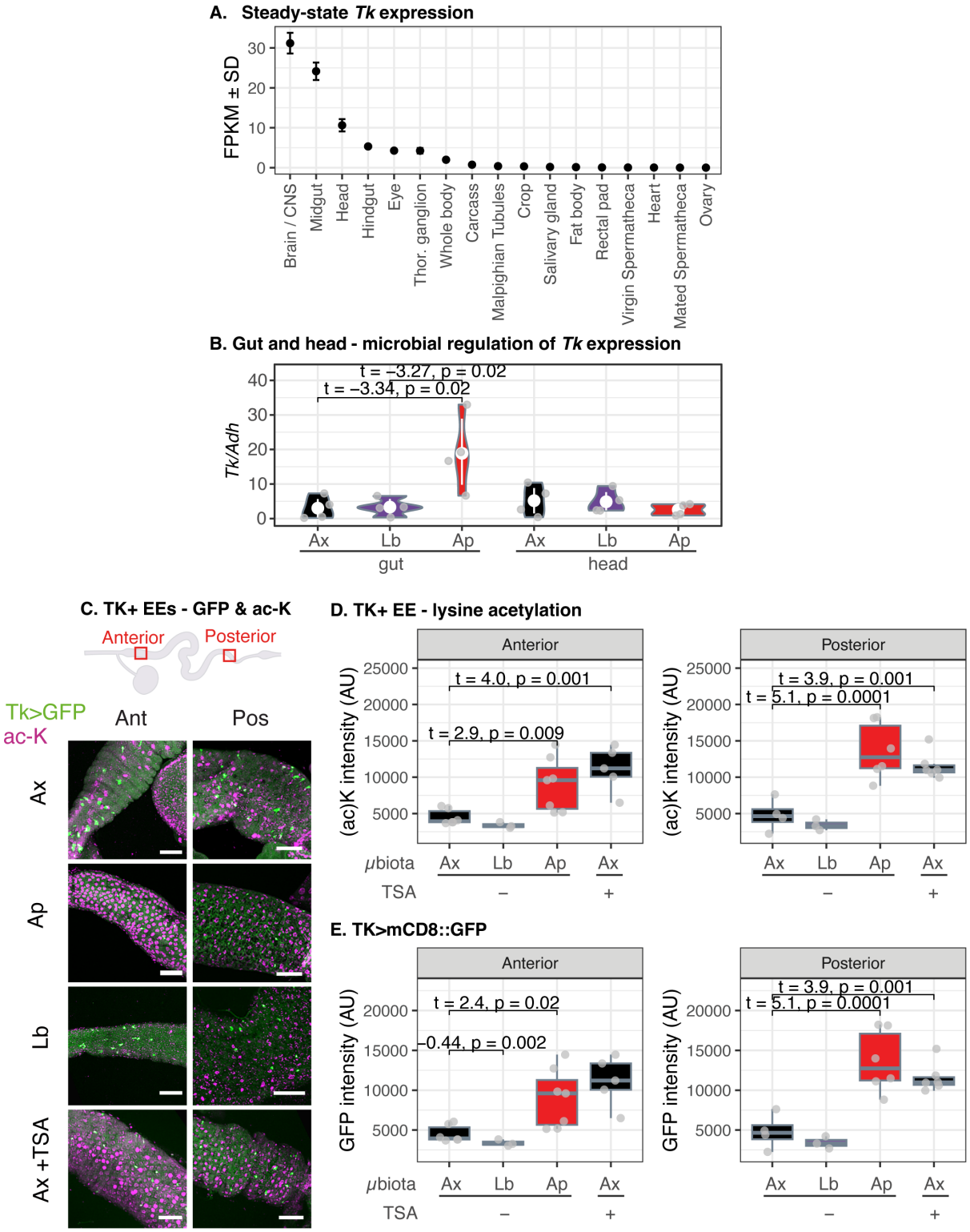

Figure 4. *A. pomorum* modulates intestinal *Tk* expression. A. *Tk* expression is enriched in nervous system and midgut tissues (data from FlyAtlas2). **B.** RT-qPCR of *Tk* in dissected midguts and heads of axenic and gnotobiotic flies indicates that expression is increased specifically in the midgut by *A. pomorum,* but not in the head; while *L. brevis* affects expression in neither tissue. White point and error bars show mean±SD. Statistics on brackets are from *post-hoc* EMM analyses of linear models, when significant differences were detected. **C.** Quantifying lysine acetylation and *Tk* promoter activity in *Tk*+ cells. Cartoon shows regions quantified in *Tk-Gal4/UAS-mCD8::GFP* flies with acetyl-lysine staining.

260 Scale bars=50μm. **D.** Lysine acetylation is increased specifically by *A. pomorum* in *Tk+* enteroendocrine
261 cells. Each point represents average fluorescence intensity for acetyl-lysine staining of ≥3 cells (marked
262 by *Tk>GFP*) per gut, in anterior and posterior regions. The HDAC inhibitor Trichostatin-A was fed to
263 axenic flies to confirm that increased histone acetylation is detectable by total acetyl-lysine staining.
264 Statistics from one-way ANOVA, showing comparisons relative to axenic control condition. **E.** *A.*
265 *pomorum* increases *Tk* promoter activity (*Tk-T2A-Gal4>UAS-GFP*) in anterior but not posterior midgut.
266 Each point represents average GFP intensity of ≥3 cells per gut, in anterior and posterior regions.
267 Statistics from one-way ANOVA, showing comparisons relative to axenic control condition.
268
269 **Intestine-directed *Tk* knockdown abrogates lifespan impact of *A. pomorum***
270 Next we asked whether *Tk* knockdown specifically in the gut blocked the shortened lifespan of *Ap*-flies,
271 using the *Gal4-UAS* system. In the midgut, EEs are marked by *voila-Gal4*, but this construct is also
272 expressed in some neurons [48,49] , posing a challenge for fully parsing effects of neurons versus midgut
273 EEs. We used a recently-developed intersectional strategy, in which *ChAT-Gal80* represses neuronal
274 *voila-Gal4* [50], directing Gal4 to the midgut while sparing CNS. After confirming that this system was
275 effective in our lab's genetic background (Figure S5), we tested whether intestine-directed Tk^{RNAi}
276 abrogated impact of *A. pomorum* on lifespan, including every possible combination of *Voila-Gal4*,
277 *ChAT-Gal80*, and *UAS-*Tk^{RNAi} in a fully-factorial design (Figure 5A-B). *Ap*-flies were shorter-lived without
278 Tk^{RNAi}, but gut-directed Tk^{RNAi} abrogated this effect on lifespan. *A. pomorum* had no effect on lifespan
279 in flies expressing Tk^{RNAi} in all *voila+* cells (without *ChAT-Gal80*). Adding *ChAT-Gal80* restored a small
280 effect of microbiota, but the magnitude of effect (Z-score) was diminutive, only ~27-40% of that
281 observed in controls. A second CoxPH analysis of the same data confirmed an overall 4-way interaction
282 of *A. pomorum* and the three transgenes, confirming that the impact of *A. pomorum* was contingent on
283 activation of Tk^{RNAi}, and the tissues in which it was activated (p=0.0005). These analyses indicated that
284 *Tk* in *Voila+* cells was obligately required for *A. pomorum* to modulate lifespan, and that the majority of
285 this effect was explained by the intestine.
286
287 For further validation we conducted a second lifespan experiment, using independent genetic tools [24]
288 to direct Tk^{RNAi} specifically to *Tk+* EEs, with *Gal4* expressed from the *Tk* locus (*Tk-T2A-Gal4*),
289 recombined with a transgene expressing *Gal80* under control of a fragment of *nSyb* promoter (*R57C10-*
290 *Gal80*), which is expected to lead to pan-neuronal *Gal80* expression as another means to attenuate
291 neuronal Gal4 activity [24,51,52]. We again detected an *A. pomorum*-by-genotype effect (Figure 5C-D), with
292 the impact of *A. pomorum* attenuated by *Tk* knockdown, and post-hoc tests showing only a marginal
293 effect of *A. pomorum* on lifespan upon Tk^{RNAi} induction (p=0.08). Independent *Gal4* and *Gal80*
294 transgenes therefore corroborated the finding that intestinal *Tk* is required for the majority of *A.*
295 *pomorum*'s lifespan-shortening effect.

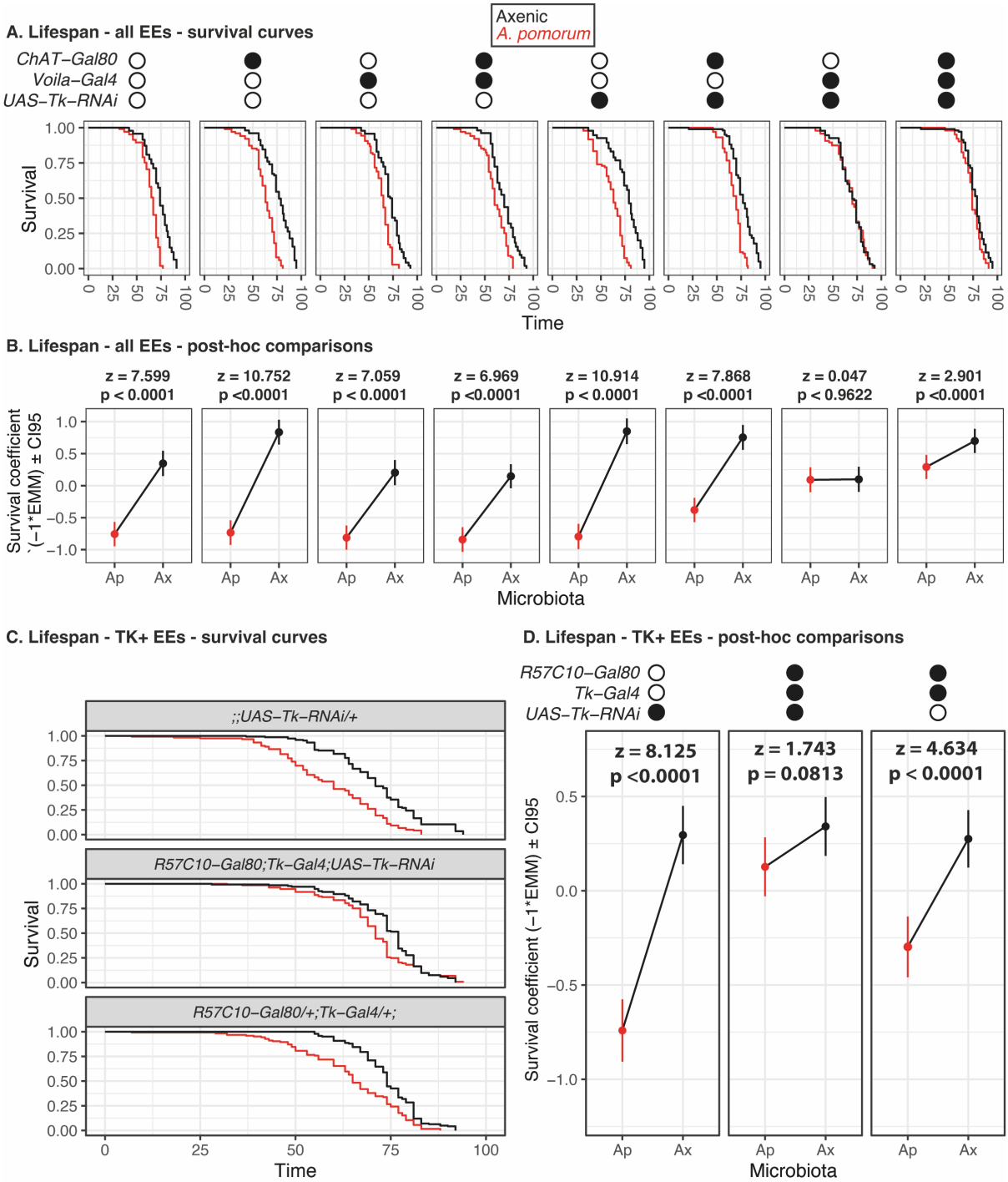

Figure 5. Gut-directed *Tk*^{RNAi} abrogates lifespan shortening by *A. pomorum*. A. Kaplan-Meier survival plots of the indicated genotypes in presence/absence of *A. pomorum*, with knockdown activated by *Voila-Gal4,* in presence/absence of *ChAT-Gal80*. Statistics from *post-hoc* tests of CoxPH model. Genotypes indicated above panels. See Figure S5 for tissue-specificity of transgene combinations. **B.** *Post-hoc* analysis of survival model reveals attenuated lifespan response to *A. pomorum* with midgut-directed *Tk*^{RNAi} (Genotypes as in A). Text indicates differences between *A. pomorum* and axenic flies in the given genotype. CoxPH analyses detected significant interactions both for microbiota*genotype (p<2.2e-16) and for Microbiota*:Voila-Gal4:ChAT-Gal80:UAS-TkRNAi* (p=0.0005). **C.** Kaplan-Meier survival plots of the indicated genotypes in presence/absence of *A. pomorum*, with knockdown activated

306 by *Tk-T2A-Gal4,* and neuronal activity suppressed by *R57C10-Gal80*. **D.** *Post-hoc* analysis of survival
307 model reveals attenuated lifespan response to *A. pomorum* with *Tk*^{RNAi} directed to midgut by *Tk-T2A -*
308 *Gal4* and *R57C10-Gal80*. Statistics from *post-hoc* tests of CoxPH model, indicating differences between
309 *Ap*-flies and axenic flies in the given genotype. CoxPH detected overall genotype-by- *A. pomorum*
310 interaction (p=2.46e-5).
311
312
313 **Role for neuronal *TkR99D*^{RNAi} in host ageing effects of *A. pomorum***
314 We asked which receptors might mediate the *Tk*-dependent response to *A. pomorum*, and from which
315 tissues. The fly genome expresses two cognate Tk receptors (TkRs) - *TkR86C* and *TkR99D* - which
316 have different affinities for the six peptides encoded by *Tk* [53], and distinct physiological roles. Plotting
317 steady-state (microbiota-independent) *TkR86C* and *TkR99D* expression, again using FlyAtlas2 data [46],
318 revealed that both TkRs were most strongly expressed in CNS (Figure 6A). We expected that knocking
319 down either one or both TkRs should extend lifespan in *Ap*-flies, mimicking effects of *Tk* knockdown.
320
321 We tested the lifespan impacts of adult-onset TkR manipulation. RNAi constructs were developmentally
322 lethal when crossed to ubiquitous drivers (*DaGS* and *ActGS*), even in the absence of inducer (RU), so
323 instead we established lifespan experiments using the pan-neuronal driver, *Elav-GS*. RNAi against
324 each TkR interacted with the lifespan effect of *A. pomorum*, but in notably distinct ways. *TkR86C*^{RNAi}
325 did not impact lifespan in *Ap*-flies, but axenics were no longer long-lived (Figure 6B-C): this reveals an
326 interaction with *A. pomorum* but does not recapitulate that of *Tk*^{RNAi}*,* suggesting that TkR86C likely does
327 not signal downstream of the *A. pomorum-Tk* relay. By contrast, *TkR99D*^{RNAi} rendered *Ap*-flies flies
328 long-lived, equivalent to axenics (Figure 6D-E). The most parsimonious explanation of these results is
329 an *Acetobacter*-Tk-TkR99D relay, which shortens lifespan.
330
331 In fly midgut, TkR99D reportedly plays a role in mobilising lipid stores in enterocytes of the fly midgut
332 [25], prompting us to ask whether it may play an additional role in lifespan from these cells. However,
333 expressing *TkR99D*^{RNAi} with the *Mex-GS* driver did not extend *Ap*-flies lifespan, suggesting that the *A.*
334 *pomorum*-Tk relay signals gut-nonautonomously (Figure S6).
335
336 Finally, we asked whether lifespan extension in axenics and upon knockdown of *TkR99D* was
337 accompanied by improved health in older flies (i.e. healthspan). Fly microbiota compromise healthspan
338 by promoting gut barrier dysfunction in aged animals, characterised by permeability which shortly
339 precedes death [54–57] . We therefore tested whether *A. pomorum* promoted gut barrier dysfunction, and
340 whether this could be rescued by *TkR99D*^{RNAi} induction. We aged axenic and *Ap*-flies, with *TkR99D*^{RNAi}
341 from day 3 of adulthood onwards, before feeding on a blue dye to report gut permeability after 56 days
342 (Figure 6F). *Ap*-flies indeed exhibited a higher rate of gut permeability than axenics, but *TkR99D*^{RNAi}
343 rescued the pathology to a level that was not significantly different from axenics. Thus, *TkR99D*^{RNAi} can

344 ameliorate deleterious impacts of *A. pomorum* on late-life health, suggesting that the putative *A.*
345 *pomorum-Tk-TkR99D* relay limits late-life health.
346

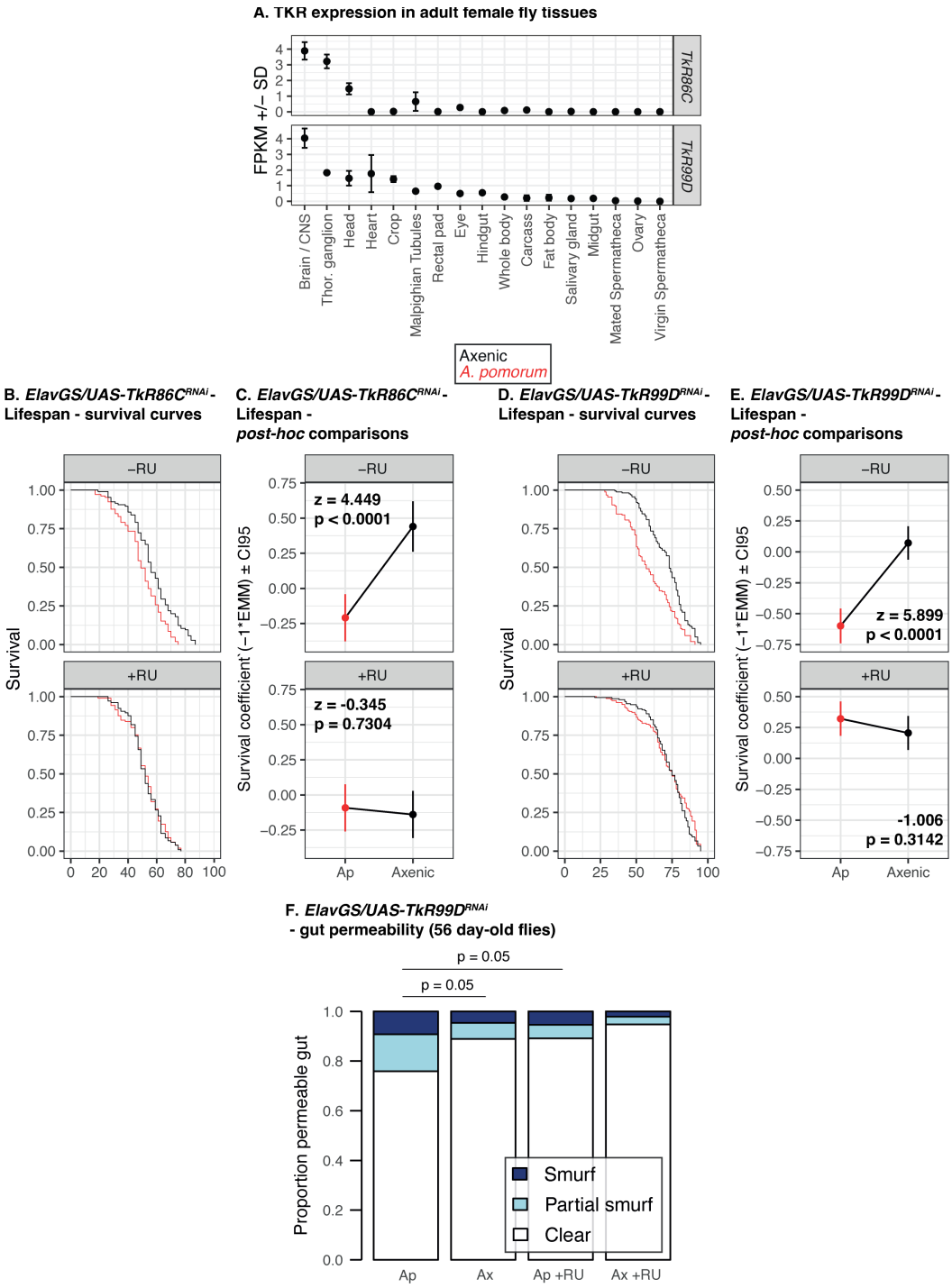

347
348 **Figure 6. Pan-neuronal *TkR99D*^{RNAi} abrogates lifespan impact of *A. pomorum*. A.** FlyAtlas data
349 showing expression of the two cognate *Drosophila* Tk receptors, *TkR86C* and *TkR99D*, among adult
350 female tissues. **B.** Kaplan-Meier survival plots of *Elav-GS; UAS-TkR86C*^{RNAi} flies in presence/absence
351 of *A. pomorum*, with knockdown activated by RU486 feeding (bottom facet). CoxPH detected significant
352 microbiota*RU interaction (p=0.0005). **C.** Post-hoc analysis of data from B showing that *TkR86C*^{RNAi}
353 induction locks axenic flies into a shortened lifespan. Text indicates differences between *A. pomorum*

354 and axenic flies in each given RU condition. **D.** Kaplan-Meier survival plots of *Elav-GeneSwitch; UAS-*
355 *TkR99D*^{RNAi} flies in presence/absence of *A. pomorum*, with knockdown activated by RU486 feeding
356 (bottom facet). CoxPH detected significant microbiota*RU interaction (p=1.362e-6). **E.** Post-hoc
357 analysis of data from B showing that *TkR99D*^{RNAi} induction blocks shortening of lifespan by *A. pomorum*.
358 Text indicates differences between *A. pomorum* and axenic flies in each given RU condition. **F.**
359 Neuronal *TkR99D*^{RNAi} blocks onset of gut permeability ("smurf" phenotype) in aged flies. Bars show
360 relative frequencies of flies with blue dye appearing to permeate through all tissues ("full smurf") and
361 through abdomen/thorax ("partial smurf"). χ^2=16.126, DF=6, p=0.013. P-values on figure from chi-
362 square tests of each given pair of columns, shown when differences were observed (otherwise omitted).
363
364 **Lifespan and metabolic impacts of *A. pomorum* are not explained by *TkR99D* in insulin-**
365 **producing cells**
366 What happens downstream of the putative *A. pomorum*-Tk-TkR99D relay? Reduced insulin signalling
367 promotes healthy ageing across species, with lifespan and other benefits reported in flies, nematodes
368 and rodents, and genetic associations indicating potential conservation in humans [58–61] . *A. pomorum*
369 is reported to activate insulin signalling [62], while *TkR99D* expression is reported in insulin-producing
370 cells (IPCs) in the fly brain [63] , ablation of which extends lifespan [64,65]. We therefore hypothesised that
371 Tk-TkR99D signalling impacts ageing by serving as a relay between the gut microbiota and IPCs (Figure
372 7A).
373
374 We tested whether insulin signalling was required for lifespan to respond to *A. pomorum*. The forkhead
375 box-O transcription factor dFOXO, encoded by the *dFoxO* locus, is obligately required for longevity
376 upon reduced insulin signalling [66,67] . We recombined a dFOXO null mutation (*dFoxO*$^{\Delta 94}$) with
377 transgenes to knock down *Tk* ubiquitously, performed lifespan assays, and used Cox proportional
378 hazards analysis to test for an *A. pomorum**Tk*dFoxO* interaction (Figure 7B-C). We observed a
379 significant three-way interaction (CoxPH p=5.384e-05) – indicating that *dFoxO*$^{\Delta 94}$ modulated the
380 microbiota-*Tk* interaction – and then used post-hoc tests to dissect the co-dependence of the three
381 experimental variables (Table 1). Without *Tk* knockdown, *dFoxO*$^{\Delta 94}$ flies exhibited a diminished but still-
382 significant shortening of lifespan by *A. pomorum*. Without *dFoxO*$^{\Delta 94}$*, Tk* knockdown blocked lifespan
383 response by rendering *Ap*-flies long-lived. In the *dFoxO*$^{\Delta 94}$ background*, Tk* knockdown did not extend
384 lifespan, in either *Ap*-flies or axenics. However, unexpectedly, *Tk*^{RNAi} ceased to block the effect of *A.*
385 *pomorum* in the *dFoxO*$^{\Delta 94}$ background. Thus, in summary, (A) *dFoxO* is partially required for lifespan
386 effect of *A. pomorum*, (B) *dFoxO* is required for lifespan extension upon *Tk* knockdown, and (C) *dFoxO*
387 is required for *A. pomorum* and *Tk* knockdown to have an interactive effect on lifespan. We interpret
388 that *dFoxO* potentiates the putative *A. pomorum*-Tk-TkR99D relay.
389

390

Table 1. *dFoxO* is partially required for microbiotaTk* interaction for lifespan: post-hoc pairwise comparisons (EMMeans)**

contrast	estimate	SE	z.ratio	p.value
(Ax WT RU-) - (Ap WT RU-)	-1.12	0.13	-8.76	6.38E-14
(Ax WT RU-) - (Ax dFoxOΔ RU-)	-0.92	0.12	-7.51	1.75E-12
(Ax WT RU-) - (Ap dFoxOΔ RU-)	-1.51	0.13	-11.87	0
(Ax WT RU-) - (Ax WT RU+)	-0.02	0.12	-0.15	0.9999999
(Ax WT RU-) - (Ap WT RU+)	-0.21	0.12	-1.77	0.63954118
(Ax WT RU-) - (Ax dFoxOΔ RU+)	-0.85	0.13	-6.79	3.21E-10
(Ax WT RU-) - (Ap dFoxOΔ RU+)	-1.48	0.13	-11.65	0
(Ap WT RU-) - (Ax dFoxOΔ RU-)	0.2	0.12	1.66	0.71153814
(Ap WT RU-) - (Ap dFoxOΔ RU-)	-0.39	0.12	-3.16	0.03369588
(Ap WT RU-) - (Ax WT RU+)	1.1	0.13	8.6	7.16E-14
(Ap WT RU-) - (Ap WT RU+)	0.91	0.13	7.27	1.00E-11
(Ap WT RU-) - (Ax dFoxOΔ RU+)	0.27	0.13	2.13	0.39332695
(Ap WT RU-) - (Ap dFoxOΔ RU+)	-0.36	0.12	-2.96	0.06098085
(Ax dFoxOΔ RU-) - (Ap dFoxOΔ RU-)	-0.59	0.12	-4.99	1.70E-05
(Ax dFoxOΔ RU-) - (Ax WT RU+)	0.9	0.12	7.34	5.87E-12
(Ax dFoxOΔ RU-) - (Ap WT RU+)	0.71	0.12	5.93	8.56E-08
(Ax dFoxOΔ RU-) - (Ax dFoxOΔ RU+)	0.06	0.12	0.54	0.99943704
(Ax dFoxOΔ RU-) - (Ap dFoxOΔ RU+)	-0.57	0.12	-4.77	5.07E-05
(Ap dFoxOΔ RU-) - (Ax WT RU+)	1.49	0.13	11.7	0
(Ap dFoxOΔ RU-) - (Ap WT RU+)	1.3	0.12	10.45	7.78E-14
(Ap dFoxOΔ RU-) - (Ax dFoxOΔ RU+)	0.65	0.12	5.35	2.43E-06
(Ap dFoxOΔ RU-) - (Ap dFoxOΔ RU+)	0.02	0.12	0.19	0.99999961
(Ax WT RU+) - (Ap WT RU+)	-0.19	0.12	-1.61	0.74370666
(Ax WT RU+) - (Ax dFoxOΔ RU+)	-0.84	0.13	-6.63	9.28E-10
(Ax WT RU+) - (Ap dFoxOΔ RU+)	-1.47	0.13	-11.49	0
(Ap WT RU+) - (Ax dFoxOΔ RU+)	-0.64	0.12	-5.23	4.63E-06
(Ap WT RU+) - (Ap dFoxOΔ RU+)	-1.27	0.12	-10.23	6.75E-14
(Ax dFoxOΔ RU+) - (Ap dFoxOΔ RU+)	-0.63	0.12	-5.14	7.52E-06

391

392

To assess directly the role of tissues reported to express *TkR99D*[63], we turned to the IPCs. We first tested whether ablating these cells by expressing the pro-apoptotic factor *Rpr* would block lifespan response to *A. pomorum*. Adult-onset *Rpr* expression, using the *Dilp2-GS* driver, extended lifespan in *Ap*-flies but not axenics, which again rendered *Ap*-flies as long-lived as axenics (Figure 7D-E), and we detected an overall microbiota*RU interaction (CoxPH p=0.003), indicating a role for IPCs in lifespan shortening by *A. pomorum*. To test whether *TkR99D* directly regulated IPC function, we expressed *TkR99D*^{RNAi} under control of *Dilp2-GS* and assayed expression of the three insulin-like peptides expressed in IPCs (*Ilp2, Ilp3, Ilp5*) by qRT-PCR of heads (Figure 7F, Table 2). *Ilp2* exhibited no response to *A. pomorum* or *TkR99D*^{RNAi}.(linear model, microbiota:RU interaction $F_{1,24}$=0.424, p=0.5) However, for *Ilp3* and *Ilp5*, *A. pomorum* promoted expression, and this effect was blocked by *TkR99D*^{RNAi} induction (linear models, microbiota:RU interactions *Ilp3* $F_{1,24}$=23.404, p=0.0001, *Ilp5* $F_{1,24}$=29.261, p<0.0001.) Specifically, *Ilp3* and *Ilp5* expression levels were increased in *Ap*-flies, but these effects were absent upon *TkR99D*^{RNAi} induction (Table 2).

Table 2. *TkR99D*^{RNAi} in insulin-producing cells blocks increased expression of *dilp3* and *dilp5*, but not *dilp2*, by *A. pomorum*: *post-hoc* tests.

Transcript	contrast	estimate	SE	df	t.ratio	p.value
dilp2	(axenic -) - (ap -)	0.34	0.82	24	0.42	0.98
	(axenic -) - (axenic +)	0.05	0.82	24	0.06	1
	(axenic -) - (ap +)	1.15	0.82	24	1.4	0.51
	(ap -) - (axenic +)	-0.29	0.82	24	-0.35	0.98
	(ap -) - (ap +)	0.81	0.82	24	0.98	0.76
	(axenic +) - (ap +)	1.1	0.82	24	1.34	0.55
dilp3	(axenic -) - (ap -)	-3.9	0.82	24	-4.74	0.0004
	(axenic -) - (axenic +)	-2.67	0.82	24	-3.24	0.02
	(axenic -) - (ap +)	-0.93	0.82	24	-1.13	0.67
	(ap -) - (axenic +)	1.23	0.82	24	1.5	0.45
	(ap -) - (ap +)	2.97	0.82	24	3.6	0.01
	(axenic +) - (ap +)	1.73	0.82	24	2.1	0.18
dilp5	(axenic -) - (ap -)	-4.18	0.82	24	-5.07	0.0002
	(axenic -) - (axenic +)	-3.32	0.82	24	-4.03	0.003
	(axenic -) - (ap +)	-1.19	0.82	24	-1.45	0.48
	(ap -) - (axenic +)	0.86	0.82	24	1.04	0.73
	(ap -) - (ap +)	2.98	0.82	24	3.62	0.01
	(axenic +) - (ap +)	2.13	0.82	24	2.58	0.07

410 Finally, we tested whether *TkR99D*^{RNAi} in IPCs restored axenic-like longevity in *Ap*-flies (Figures 7G-
411 H). As expected, *TkR99D*^{RNAi} induction in IPCs did not affect axenic lifespan, and *Ap*-flies were shorter-
412 lived than axenics without *TkR99D*^{RNAi}, but, surprisingly, the lifespan-shortening effect of *A. pomorum*
413 was exaggerated by *TkR99D*^{RNAi} induction (Figure 7H). The lifespan-shortening effect of *A. pomorum*
414 therefore seemingly cannot be explained by activating signalling through TkR99D in IPCs. We also
415 tested whether *TkR99D*^{RNAi} in IPCs altered effects of *A. pomorum* on TAG levels in young flies (Figure
416 7I): no interaction was apparent (though we detected independent effects of microbiota (ANOVA
417 F=14.95, Df=1,37, p=0.0004) and RNAi induction (F=4.32, Df=1,37, p=0.04)), suggesting that
418 interactive effects of *A. pomorum* and Tk peptides are not mediated by *TkR99D* in IPCs.
419
420 Altogether, these data outline involvement of insulin signalling in responses to *A. pomorum* and *Tk*, but
421 they do not suggest an obligate requirement for insulin signalling directly downstream of *A. pomorum*-
422 Tk-TkR99D signalling.
423

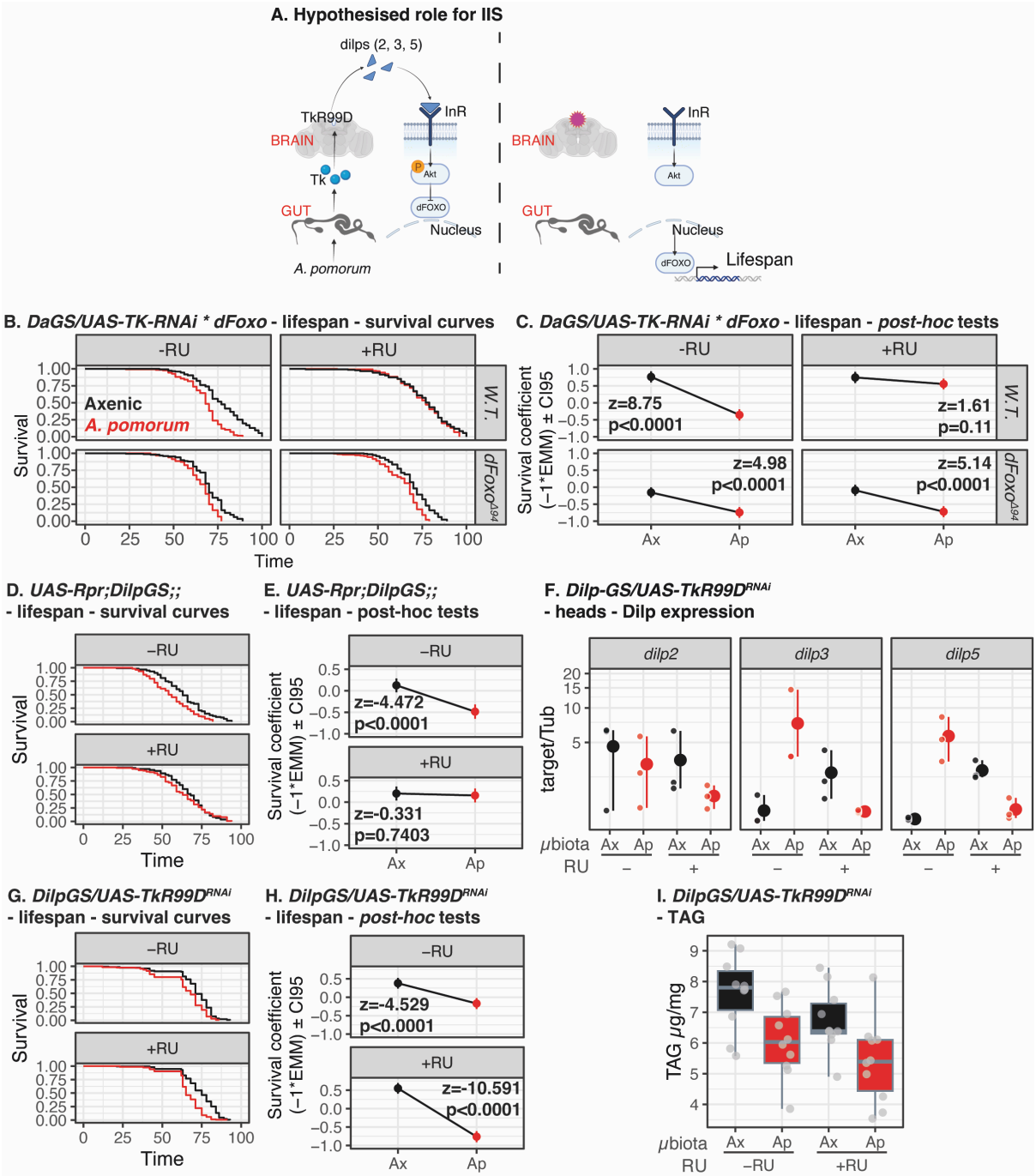

Figure 7. Insulin signalling is involved in lifespan response to *A. pomorum* and *TkR99D* knockdown, but not obligately required. A. Hypothetical model of role for IIS. In presence of microbiota (left), Tk peptides are released from gut and contact TkR99D in IPCs/brain. IPCs are released into circulation, activating insulin signalling in peripheral tissues and leading to nuclear exclusion of dFOXO. In absence of microbiota (right), extracellular signalling is diminished, reducing downstream insulin signalling and consequent activation of lifespan-extending gene expression program by dFOXO. **B.** dFOXO connects lifespan responses to *A. pomorum* and ubiquitous Tk^{RNAi}. Facets show Kaplan-Meier plots in axenic and *A. pomorum* conditions, with/without RNAi induction (RU), and with/without $dFoxO^{\Delta 94}$ null mutation**.** Overall microbiota*RU*Foxo interaction p=5.384e-05 (CoxPH) **C.** Post-hoc comparisons (EMmeans), showing impact of *A. pomorum* under specified

435 conditions of *TkRNAi* induction and *dFoxO* deletion. *A. pomorum* shortens wild-type lifespan, but this
436 effect is diminished by *dFoxO*$^{\Delta 94}$. *Tk*^{RNAi} induction blocks lifespan shortening by *A. pomorum* in wild-
437 type background, but not in *dFoxO*$^{\Delta 94}$ background; altogether suggesting that *dFoxO* is required for *A.*
438 *pomorum* to influence longevity via Tk modulation. **D-E.** Insulin-producing cells (IPCs) are required for
439 *A. pomorum* to influence lifespan (CoxPH p=0.003). Post-hoc tests (**E**) confirm that lifespan effect of *A.*
440 *pomorum* (-RU) is absent following IPC ablation (*Rpr* expression, +RU). **F.** *A. pomorum* increases
441 expression of *Dilp3* and *Dilp5,* but not *Dilp2*, in a *TkR99D* -dependent manner. Panels show expression
442 (RT-qPCR) in heads of axenic and *Ap*-flies ±*TkR99D*^{RNAi} in IPCs (*Dilp2-GS/UAS-TkR99D*^{RNAi}). by
443 Microbiota*RU interactions were tested for with linear models: *Dilp2* $F_{1,24}$=0.424, p=0.5, *Dilp3*
444 $F_{1,24}$=23.404, p=0.0001, *Dilp5* $F_{1,24}$=29.261, p<0.0001. **G-H.** *TkR99D*^{RNAi} in IPCs worsens lifespan
445 impact of *A. pomorum*. (**I**) Post-hoc tests indicate accentuated shortening of lifespan by *A. pomorum*
446 following *TkR99D*^{RNAi} induction (+RU). **I.** *TkR99D*^{RNAi} in IPCs does not modulate metabolic impact of *A.*
447 *pomorum* on fly TAG. The two experimental factors each had significant effects on TAG (ANOVA, *A.*
448 *pomorum* F=14.95, Df=1,37, p=0.0004; RU F=4.32, Df=1,37, p=0.04), but no interaction was detected.
449
450 **No evidence of role for *TkR99D* in Akh-producing cells in lifespan and metabolic response to *A.***
451 ***pomorum***
452 In insects, adipokinetic hormone (Akh) is released from *corpora cardiaca* (cc) to promote lipid
453 mobilisation in response to heightened energy demand, analogous to glucagon in mammals[68–70] .
454 Having observed *Tk*-dependent effects of microbiota on TAG storage, and following recent evidence
455 that *TkR99D* in Akh-producing cells limits lifespan[24], we tested whether it may also mediate lifespan
456 impact of *A. pomorum*.
457
458 First, to test whether Akh peptide levels in CC were *A. pomorum*-dependent, we quantified Akh with
459 antibody staining. Akh staining levels were significantly higher in CC dissected from *Ap*-flies than
460 axenics (Figure 8A), suggesting microbial regulation of Akh signalling.
461
462 We then tested directly whether TkR99D was required in Akh-producing cells for *A. pomorum* to shorten
463 lifespan. Expressing *TkR99D*^{RNAi} under control of *Akh-Gal4* did indeed extend lifespan relative to
464 controls (noting background effects, despite backcrossing immediately before experimentation), but
465 RNAi did not alter the lifespan-shortening effect of *A. pomorum* (Figure 8B-C). These data corroborate
466 a recent report that *TkR99D* knockdown in CC extends lifespan[24], but indicate that effects of *A.*
467 *pomorum* are independent of these signalling changes. We also tested whether RNAi against Akh
468 receptor (*AkhR*) in adipose (fat body) altered response to *A. pomorum*, driving expression with *S106-*
469 *GS*, but again no interaction was apparent (Figure S7). Finally, we tested whether *TkR99D* in Akh-
470 producing cells interacted with effects of *A. pomorum* on TAG storage. *TkR99D*^{RNAi} induction did not
471 block response to *A. pomorum*, with *Ap*-flies storing less lipid than axenics independent of fly genotype
472 (Figure 8D), indicating that *A. pomorum*'s influence on TAG does not depend on TkR99D in CC.

473 Combined with our investigation of insulin signalling, our studies of Akh suggest that the impact of
474 *Acetobacter* on ageing is mediated by non-canonical mechanisms that depend on *Tk* and *TkR99D.*
475

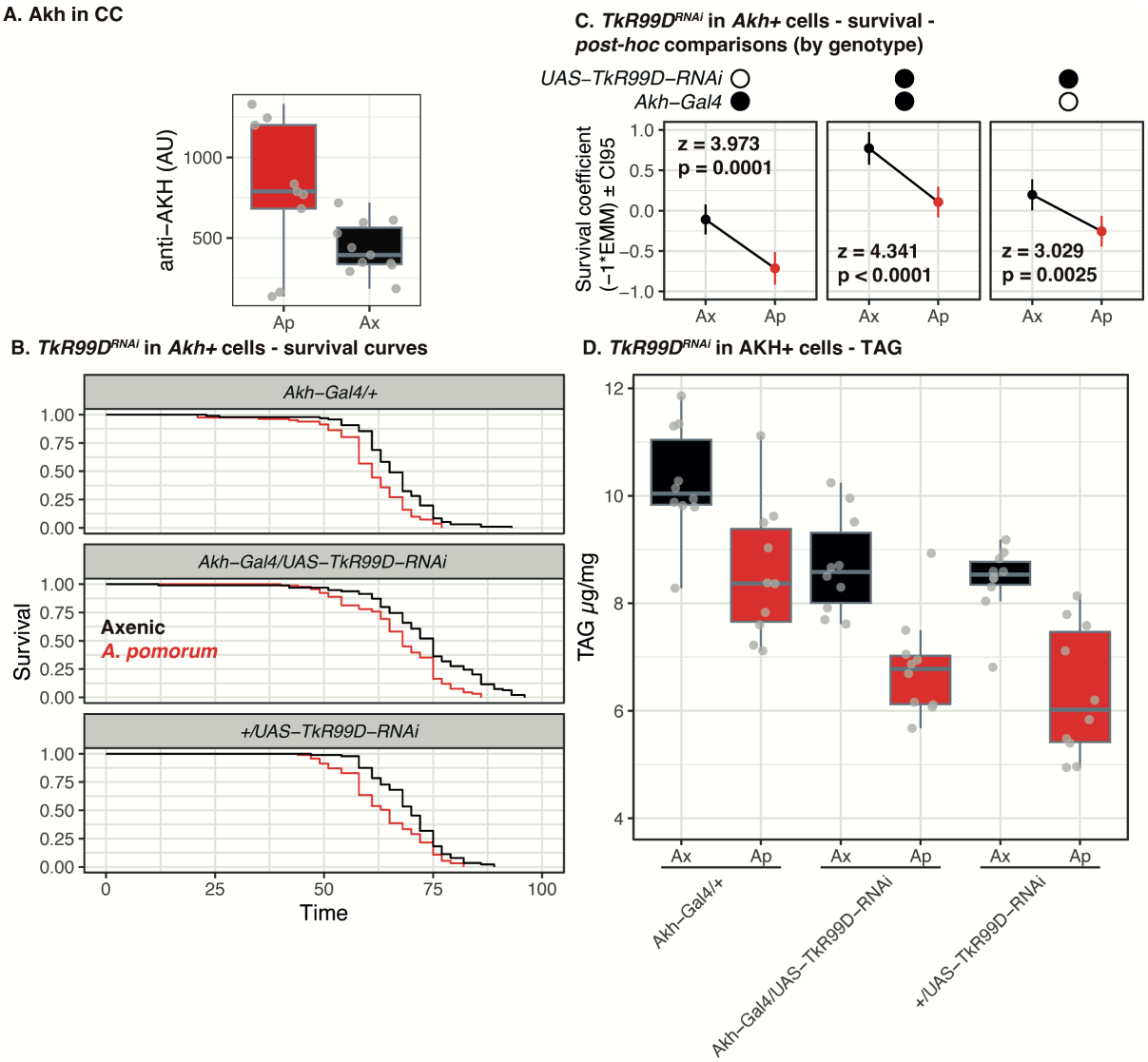

476
477 **Figure 8. *A. pomorum* modulation of host lifespan and TAG is independent of *TkR99D* in Akh-**
478 **producing cells. A.** Antibody staining of Akh in dissected Corpora Cardiaca (CC) is increased in *Ap*-
479 flies (Ap) relative to axenics (Ax). (t-test: t = -2.36, p-value = 0.04). **B.** Microbial shortening of lifespan
480 is independent of *TkR99D* signalling in Akh+ cells. Facets show Kaplan-Meier survival curves for axenic
481 and *Ap*-flies when *TkR99D* is knocked down (middle facet) and in each control genotype. No significant
482 interaction of genotype and *A. pomorum* was detected (CoxPH p=0.58). **C.** Post-hoc comparisons
483 (EMmeans) confirm equivalent lifespan shortening by *A. pomorum*, independent of
484 *TkR99D*^{RNAi}. Combination of transgenes indicated above facets. **D.** *A. pomorum* modulation of host
485 TAG is independent of *TkR99D*^{RNAi} in Akh+ cells. Boxplots show TAG levels are reduced independent
486 of *TkR99D*^{RNAi} induction. No significant interaction of genotype and *A. pomorum* detected.
487
488

489

490 ## Discussion

491 Microbiota impact ageing across animals [1,4,8,10,12,71,72], and connections between gut and the nervous
492 system are key to health throughout the lifecourse [73–75] . Here we have connected microbial regulation
493 of ageing with tissue-specific regulation of endocrine signalling genes in gut and neurons. Our
494 *Drosophila* results show that (A) *A. pomorum* is sufficient to modulate *Tk* in the midgut, (B) knocking
495 down the peptide in midgut blocks the lifespan response to the bacteria, and (C) neuronal knockdown
496 of the receptor *TkR99D* recapitulates these effects. We are struck by the specificity of this circuit, with
497 knockdown of a single peptide-encoding locus in a specific tissue ablating the microbial impact on
498 lifespan, despite the wide array of host functions that the microbiota affect. This specific requirement
499 can likely be explained by the highly pleiotropic functions of Tachykinins [31,53], suggesting that *Tk*
500 knockdown reprograms organismal physiology to a state in which lifespan can no longer be modulated
501 by microbiota. Given the evolutionary conservation of tachykinins, it will be interesting in future work to
502 ask whether this family of peptides can also modulate ageing in other species.

503

504 Our work indicates that the influence of the microbiota-*Tk/TkR99D* relay is partially independent of
505 better-studied lifespan assurance mechanisms, i.e. insulin signalling, and phenotypes associated with
506 ageing. The lifespan benefit of *Tk* knockdown was not accompanied by costs to fecundity or feeding
507 rate in CR flies, but instead knockdown altered metabolic impact of microbiota. Furthermore, knocking
508 down *TkR99D* in major signalling hubs associated with ageing and TAG metabolism (IPCs and Akh+
509 cells, respectively) did not block lifespan or TAG response to *A. pomorum*, suggesting that yet-
510 uncharacterised neuroendocrine mechanisms are at play. We interpret the partial requirement for
511 *dFoxO*, connecting *A. pomorum* to Tk^{RNAi} modulation of lifespan, as suggesting that insulin potentiates
512 downstream responsiveness, without necessarily being involved directly by *TkR99D* in IPCs.

513

514 Our work was performed entirely in females. We chose to study the sex that tends to exhibit more robust
515 response to anti-ageing interventions[76] , because of the labour-intensive and technically challenging
516 nature of performing lifespan experiments under lifelong axenic conditions. Having established this the
517 *A. pomorum-Tk-TkR99D* connection, it will be interesting in future work to ask whether males also enjoy
518 a lifespan benefit of diminishing the activity of this circuit.

519

520 *Tk* is one of a number of signalling circuits implicated downstream of the microbiota, for example JAK-
521 STAT and JNK signalling[77] , IMD[47,78] , and the neuropeptide CNMamide [79]. We do not propose that
522 Tachykinins alone are sufficient to explain all physiological effects of the microbiota: rather we expect
523 that the interplay of multiple signalling pathways collectively orchestrate the host organismal response
524 to microbiota. Indeed our transcriptome (re)analysis (Figure 1B) suggested that a community of bacteria
525 co-regulate expression of the neuropeptides *ITP, AstC* and *NPF* alongside *Tk.* We note that *Tk* and
526 *NPF* are co-expressed in a number of the same EE populations[80], and related functions on nutrient-

527 specific appetite, physiology and Akh signalling are reported[51,81] , suggesting closely coupled functions
528 for Tk and NPF which may also be relevant to integrating responses to microbiota. Further work should
529 aim to identify the broader signalling networks that respond to the microbiota, and the extent to which
530 the constituents and structure of those networks mirror what is known in other contexts (e.g. responses
531 to diet or pathogenic infection).
532
533 A key element to better understanding how signalling networks at large respond to microbiota will be to
534 better understand what properties of the microbiota the signals convey. Signalling is selected to convey
535 information about environmental, nutritional, and physiological state: which of these parameters do the
536 microbiota impact? Impacts on metabolism could be mediated by direct provision of nutrients (e.g.
537 short-chain fatty acids, B-vitamins[4,26,82]), and/or competition with the host by removal of nutrients from
538 diet[83] . Immunity may be modulated by bacterial titre, to prevent pathological overgrowth of otherwise
539 mutualistic bacteria. Our results indicate that the interplay between bacteria and *Tk* knockdown is
540 bacteria-specific, suggesting in turn that more complex mixes of bacteria that co-occur with the fly may
541 elicit distinct signalling network topologies. Furthermore, the previous finding that fly transcriptional
542 networks are structured by microbiota[84] lead to a question of whether other host networks - such as
543 endocrine signalling - may also be structured by microbiota, in which case signalling in the presence of
544 one bacterium might elicit quite different physiological responses than in the presence of a distinct
545 bacterium.
546
547 The two biggest mechanistic questions arising from this work are (A) from where in the nervous system
548 does *TkR99D* inhibition extend lifespan? and (B) by what mechanism does inhibition extend lifespan?
549 We tested two neuroendocrine tissues, the IPCs and the Akh+ cells, finding that *TkR99D*^{RNAi} in either
550 did not block shortened lifespan or TAG phenotypes in *Ap*-flies (though bacteria-independent effects of
551 *TkR99D*^{RNAi} in *Akh+* cells were apparent). These data suggest that we can reject a role for TkR99D in
552 IPCs and *Akh+* cells, and instead that an elusive population of *TkR99D+* neurons is at play downstream
553 of the *Acetobacter-Tk* relay. With respect to future mechanistic understanding, we suggest it will be
554 important to note that pan-neuronal *TkR99D*^{RNAi} also mitigated gut permeability (smurfing) in aged *Ap*-
555 fies, because the smurf phenotype is underpinned by increased immune system activity[56,85] , and
556 activation of *Tk* cells by *Acetobacter* is dependent on immune (IMD) signalling[47]. Together these
557 observations suggest close links between *Tk* signalling and immunity, outlining a possible role for
558 *Acetobacter/Tk/TkR99D* in "inflammaging".
559
560 The biggest comparative question arising from our work is whether our findings are relevant in other
561 animals, potentially including mammals. Flies have a track record of revealing mechanisms of ageing
562 that are conserved in other systems[58–60,86–90]. Tachykinins are conserved from invertebrates to
563 mammals, raising the question of whether their functions in ageing are also conserved. The next step
564 would most likely be to assess whether Tachykinin knockdown has anti-ageing effects in rodents, and/or
565 short-lived vertebrates like the African turquoise killifish. Such studies may pave the way for drug

566 repurposing, as some small-molecule inhibitors of human TkRs have already been developed and are
567 licenced in some jurisdictions for specific purposes. Such interest is timely since the therapeutic role of
568 TkRs is receiving renewed attention for potential metabolic therapies[91].
569
570 In conclusion, our study establishes a mechanistic connection between the microbiota and ageing via
571 gut/neuron signalling. Microbial lifespan effects depend on *Tk/TkR* signalling, which can be explained
572 by *Acetobacter* activating intestinal *Tk* and, downstream, neuronal *TkR99D*. The findings hint at effects
573 which may be conserved in other systems, which may ultimately help to explain mechanistically why
574 microbiota exert a conserved influence on animal health and ageing.
575

576 ## Materials and methods

577

578 **Flies, bacteria, husbandry and culturing**

579 Stocks used are detailed in Table 3. All stocks (except for recombinant *R57C10-Gal80;;Tk-T2A-Gal4,*
580 gift from Kim Rewitz) were backcrossed into the Dahomey background (originally isolated from Benin
581 in the 1970s), bearing the *w1118* mutation and confirmed *Wolbachia*-negative. Presence of $dFoxO^{\Delta 94}$
582 in recombinant flies was confirmed by PCR of mothers of single-fly crosses.

583 All flies were maintained at 25°C with a 12-12-hour light- dark cycle on SYA medium, comprising 5%
584 sucrose (MP Biomedicals BP220), 10% yeast (MP Biomedicals, 903312, lot no. S7760), and 1.5% agar
585 (Sigma-Aldrich A7002)[92,93]. Preservatives (0.3% nipagin, 0.3% propionic acid) were incorporated into
586 media for stock maintenance. Crosses were performed on juice agar in egg laying cages (per litre: 20g
587 agar, 26g sucrose, 52g glucose, 7g yeast, 88.8ml organic clementine or grape juice). To generate
588 axenic flies, eggs were collected and washed 2x in alternating 10% bleach for (3-5 min) and sterile
589 ddH2O for (1 min), with an optional additional 1 min wash in EtOH, before being allowed to pellet by
590 gravity in sterile PBS. 20 μl of egg pellet was aspirated with wide-mouthed pipette tips into T75 flasks
591 containing 50mL SYA. Preservatives were included during fly development only in CR experiments. We
592 made gnotobiotic embryos as as previously [93]. M9+lactate media comprised 200ml 5x M9 salts, 2ml
593 1M $MgSO_4$, 1ml 1M $CaCl_2$, 25ml 20% (v/v) lactate, made up to 1l in ddH_2O and autoclaved. YPD media
594 comprised 10g yeast extract (VWR 84601.0500), 20g peptone (VWR 84620.0500), 20g dextrose
595 (Fisher Life Sci G/0500/53). *Acetobacter pomorum* (DmCS004) was streaked and grown on M9+lactate
596 plates (1.5% agar), before growing single colonies in liquid M9+lactate at 30°C with shaking (225 rpm)
597 for 2 days. (DmCS004). *L. brevis* (DmCS003) was streaked on YPD (1.5% agar), then grown in liquid
598 YPD for two days at 30C in static culture. Cultures were pelleted, washed, resuspended and diluted in
599 sterile PBS to an OD_{600} of 0.2. 200 μL of bacterial suspensions were added to T75 flasks containing
600 freshly-prepared axenic eggs.

601

602 Newly emerged flies transferred to fresh media using sterile technique in a laminar flow hood,
603 (preservatives as per development) for the first three days of adulthood before gentle anaesthesia on
604 CO_2. Males were removed and females allocated to SYA containing preservatives in sterile glass
605 *Drosophila* vials, using aseptic technique in a laminair flow hood with a sterile paint brush and sterile
606 petri dish on ice. In experiments using RU486 (Mifepristone, Cayman Chemical, CAY10006317), 2ml l^{-}
607 ^{1} of 100mM RU486 stock solution in EtOH was incorporated into media at 200μM final concentration,
608 and fed from day 3 adulthood onwards. 2ml EtOH was incorporated as vehicle control in RU-free
609 controls.

610 For lifespan assays, mated females were allocated to sterile glassware in groups of 15, and transferred
611 to fresh food every 2–3 days. At each transfer, deaths and censors were scored until all flies were dead.
612 For axenic and gnotobiotic lifespans, fly tipping was performed in a sterile laminar flow hood with aseptic
613 technique.
614

615 **Table 3. *Drosophila* stocks used in this study.**

Genotype	Abbreviation	Source		
		BDSC	VDRC	Other
***UAS* lines**				
UAS-TK-shRNAi			v330743	
UAS-TK-RNAi		B25800		
UAS-TK-RNAi			v103662	
UAS-TkR99D-RNAi			v44369	
UAS-TkR86C-RNAi			v107090	
UAS-Reaper				Cathy Slack, U. Warwick
UAS-AkhR-RNAi				Kenneth Halberg, U. Copenhagen
UAS-MCD8::GFP				Julia Cordero, U. Glasgow
***Gene Switch* drivers**				
Daughterless-GeneSwitch;	***DaGS***			Cathy Slack, U. Warwick
Dilp2-GeneSwitch	***Dilp-GS***			Nathan Woodling, U. Glasgow
S106-GeneSwitch	***S106-GS***			Cathy Slack, U. Warwick
Elav-GeneSwitch	***Elav-GS***			Nathan Woodling, U. Glasgow
Mex-GeneSwitch	***Mex-GS***			Jean-René Martin, CNRS Université Paris-Saclay
***GAL4* drivers**				
Voila-GAL4				Julia Cordero, U. Glasgow
Akh-GAL4				Kenneth Halberg, U. Copenhagen
TK-T2A-GAL4	***TK-GAL4***			Kim Rewitz, U. Copenhagen
Chat-Gal80				Julia Cordero, U. Glasgow
R57C10-Gal80				Kim Rewitz, U. Copenhagen
Other				

FOXOO Δ		Cathy Slack, U. Warwick
White Dahomey-20	***wD-20***	Enric Ureña & Nazif Alic, UCL.

616

617 **Feeding and egg laying assays**

618 Feeding rate was measured by quantifying average proboscis extension rate (PER) over 3-4 hours.
619 Vials containing 5 mated females each were arranged on a benchtop in a 25ºC room the night before
620 behavioural observations to allow acclimation. Experimenters were blinded to vial ID and experimental
621 condition. The following morning, PER was recorded by iteratively counting the instantaneous number
622 of flies feeding per vial for 3-4 hours. The average of these measurements per each given vial was
623 taken as that vial's feeding rate. At the end of the experiment, flies were disposed, and vials frozen. The
624 next day eggs were counted from the same frozen vials.

625 **TAG assay**

626 Female flies were collected and divided into groups of 5, 3 days post eclosion. Each group was weighed
627 on a Thermo microbalance to an accuracy of .01 mg. Weighed females were added to a sterile 2mL
628 screw-cap tube containing sterile 1.4mm ceramic beads and 125 μL of TET buffer (10mM Tris, 1mM
629 EDTA, pH 8.0, 0.1% (v/v) Triton-X-100). Samples were homogenised for 30s at max speed. After
630 homogenisation, samples were incubated at 72°C for 15 min in a dry bath to inactivate lipases and
631 other enzymes. Then samples were centrifuged at max speed for 5 min at 4°C. From each sample 3
632 μL of the supernatant was added to a clear, flat bottom 96 well plate. Standard curves were generated
633 using a glycerol stock ranging from 1-0 ug/ul. Triglyceride levels were assayed by the method of Fossati
634 and Prencipe[94] , with absorbance measured at 540 nm in a Thermo MultiSkan FC plate reader.

635 **RNA extraction**

636 RNA was extracted from whole flies by the addition of 10 female flies per sample to sterile 2 mL screw
637 cap tubes containing 600 μL of TRIzol (Ambion by Life technologies) and homogenised in a Ribolyzer
638 and running at 6.5 (max) for 10 seconds. 200 μL chloroform was added, briefly vortexed, and incubated
639 at RT for 3 min. Samples were centrifuged 12,000rpm for 15m at 4ºC, 250μl of isopropanol was added
640 to supernatants, vortexed, and incubated at RT for 10 minutes. Samples were then centrifuged at
641 12,000rpm for 10m at 4ºC. The liquid was removed and discarded, while the pellet containing the RNA
642 was washed with 1mL of 75% ethanol. Samples were centrifuged at 12,000 rpm for 10m at 4ºC. The
643 liquid was removed without disturbing the pellet, and the tubes were dried at RT with caps opened.
644 Pellets were reconstituted in DEPC water (10μl/fly) and stored at -80ºC.
645

646 **16s amplicon sequencing**

647 DNA was extracted from whole guts, dissected from 3 day-old wild-type stock females (i.e.
648 conventionally-reared and bearing a complete microbiota, 5 per sample, 10 samples total) after 1

649 minute surface-sterilisation in 70% EtOH. Guts were deposited immediately into TRIzol and
650 homogenised in a ribolyser. 300μl chloroform was added and inverted followed by 3 mins incubation at
651 room temperature, 15 minutes centrifugation at 12000g. Aqueous layer was removed before 500μl back
652 extraction buffer (4M Guanidine thiocyanate, 50 mM sodium citrate, 1M Tris base) was added and
653 mixed by inverting. Samples were spun again at 12000g for 30 minutes and aqueous phase transferred
654 to new tubes with 400 μl isopropanol. Samples were mixed by inversion, centrifuged 15 minutes at
655 12000g. Pellets were washed in 70% ethanol, dried, and resuspended in 50 μl TE buffer.
656
657 Library prep was performed by the University of Glasgow MVLS Shared Research Facility from 12.5ng
658 input DNA per sample, with an initial PCR using Accustart PCRToughMix and 0.5μl 10mM primers
659 against 16s V3/V4 region (FWD
660 TCGTCGGCAGCGTCAGATGTGTATAAGAGACAGCCTACGGGNGGCWGCAG, REV
661 GTCTCGTGGGCTCGGAGATGTGTATAAGAGACAGGACTACHVGGGTATCTAATCC), using 25
662 cycles at an annealing temperature of 60°C, followed by barcoding with Illumina Nextera XT 1 primers,
663 cleanup with 0.9X Spri Select beads (Beckman Coulter), and washing in 80% EtOH. Libraries were
664 quantified by Qubit HS DNA assay and size distributions checked on an Agilent Bioanalyser. Pooled
665 libraries were sequenced on an Illumina MiSeq in paired end mode (300bp) using a 600 cycle cartridge
666 kit, 5% PhiX, to an average depth of 170K reads per sample.
667
668 **RT-qPCR**

669 RNA samples were quantified by spectrophotometry using a Nanodrop 1000 UV-Vis spectrophotometer
670 (ThermoScientific). First strand synthesis of cDNA was performed using the SuperScriptTM Reverse
671 Transcriptase (RT) kit (Invitrogen), following the manufacturer's protocol (using 2μg of RNA). The PCR
672 profile was as follows: 95°C for 2 minutes; 94°C denaturation for 30 seconds, 60°C annealing for 30
673 seconds, 72°C extension for 30 seconds each for 40 cycles, with a final extension at 72°C for 5 minutes.
674 The amplicon was migrated through a 1% (w/v) agarose gel. To test for relative gene expression levels,
675 RT-qPCR was performed. Each well contained 2 µl cDNA, 1.5 µl 10 mM forward primer, 1.5 µl 10 mM
676 reverse primer, 3 µl water, 10 µl SYBR green PCR master mix, and 2 ul ROX (Qiagen, UK). The
677 following PCR profile was used: 95°C for 5 minutes; 94°C for 30 seconds, 60°C for 30 seconds, 72°C
678 for 30 seconds each for 40 cycles, and a final extension at 72°C for 5 minutes. Mean cycle threshold
679 (Ct) values for duplicates of each of the studied genes were derived by subtracting the combined mean
680 Ct value of constitutively expressed housekeeping genes *alcohol dehydrogenase* (*ADH*) or *tubulin*.
681 Primers shown in Table 4.

682

683

684 **Table 4 Primers for RT-qPCR**

Target	*Forward*	*Reverse*
TK	TTCATATGCGCCCTCTGAGCG	ATGAAGCTGGACGTGGGCGC
Bursicon	CGCCACGAGAACAACAAGGT	CATCCAGGATACTGGAGCAC
ADH	GCTAACGAGTACTTGCATCTCTTC	AGACCGGCAACGAAAATCAC
Tubulin	TCGCCGTCACCGGAGTCCAT	TGGGCCCGTCTGGACCACAA
Dilp2	ATGGTGTGCGAGGAGTATAATCC	TCGGCACCGGGCATG
Dilp3	AGAGAACTTTGGACCCCGTGAA	TGAACCGAACTATCACTCAACAGTCT
Dilp5	GAGGCACCTTGGGCCTATTC	CATGTGGTGAGATTCGGAGCTA

685

686 **Antibody staining and imaging**

687 Whole guts were extracted from 10-day old female flies (axenic, gnotobiotic, and axenic on 1μM
688 TSA), and fixed in 4% paraformaldehyde for 30m in a 12 well plate. Guts were then incubated in 1 mL
689 of PBST (1X PBS with 0.1% triton X-100) overnight with slight shaking at 4ºC. PBST was carefully
690 aspirated from sample wells, and guts were then washed with 1 mL of Blocking buffer (10% 1X PBS,
691 1% triton X-100, 2.5% Normal Goat Serum) at 4ºC overnight. Blocking buffer was removed, and 0.5
692 mL of acetyl-lysine antibody (Cell Signaling Technologies 9441) diluted 1/800 in blocking buffer was
693 added to the wells, and incubated overnight at 4ºC with slight shaking. Guts were then washed 3X
694 with PBST for 10 minutes, followed by a 1 hr RT PBST wash with slight shaking. 0.5 mL of secondary
695 antibody secondary antibodies diluted 1/200 in PBST was added to the guts, and incubated overnight
696 at 4ºC. Guts were washed 3X in PBST for 10 minutes. Guts were then mounted in Vectashield for
697 imaging.

698 Corpora cardiaca were dissected, fixed and washed as above, stained with anti-Akh (gift from
699 Kenneth Halberg) diluted 1:1000, and stained with secondary antibodies as above.

700 **Confocal microscopy**

701 Imaging was performed on a Zeiss LSM 880 confocal microscope and processed using Zeiss Zen
702 Blue (v3.8) and NIH ImageJ software 1.53a prior to transfer to Adobe Photoshop and Illustrator
703 (Creative Cloud 2025; CA, USA) for final presentation.

704 **Data analysis**

705 All enumerated data were plotted and analysed in R 4.4.2. [95]. Kaplan-Meier curves were plotted with
706 survminer::ggsurvplot_facet. Other quantitative data were plotted with ggplot2. Survival data were
707 analysed with CoxPH models (survival::coxph). Fecundity data were analysed with negative binomial

708 models (lme4::glmer.nb). All other data were analysed with stats::lm (after logit transformation for
709 proportion flies feeding). Post-hoc tests were performed with emmeans::joint_tests and
710 emmeans::pairs, coefficients were extracted from emmeans::emmip. Survival indices were generated
711 by applying emmeans::emmip to coxph models, multiplied by -1, such that higher values corresponded
712 to longer lifespan.

713 Published transcriptome data [23] were reanalysed by FastQC and quantified with Salmon. The
714 previous publication by Bost et al[23] presented bulk RNAseq on midguts of flies reared under axenic
715 conditions or with a 5-species gnotobiotic microbiota comprising *Acetobacter* and *Levilactobacillus*
716 species. The original analysis presented excluded expression of ~70% of genes in the fly genome,
717 and hormones were largely excluded. We reanalysed the raw data using Salmon [96] to quantify
718 expression, which quantified expression of 10,290 genes, including 14 of the 15 enteroendocrine
719 hormone genes (except *bursicon*). We tested for differential expression using DESeq2, identifying 470
720 differentially expressed genes (FDR ≤ 0.01, ≥2-fold difference in mean expression). These 470 genes
721 included four peptide hormones: *Tachykinin (Tk), Allostatin C (AstC), Ion Transport Peptide (ITP), and*
722 *Neuropeptide F (NPF)*. Since *Burs* was not quantified by the Salmon algorithm, we tested
723 independently whether its expression was modulated by microbiota by extracting RNA from midguts
724 of CR and axenic flies.

725 **Acknowledgments**
726 We thank Julia Cordero for helpful discussion, reagents and training; Nathan Woodling and Colin
727 Selman for comments on the manuscript; and Kim Rewitz, Kenneth Halberg, Jean-René Martin and
728 Peter Newell for reagents. The authors gratefully acknowledge the Cellular Analysis Facility at the
729 University of Glasgow – particularly David McGuinness – for support and assistance in this work. This
730 work was funded by a UKRI Future Leaders Fellowship (MR/S033939/1 and MR/Y019660/1, AD),
731 BBSRC (BB/W510658/1, DRS and AD), a University of Glasgow Lord Kelvin Adam Smith Fellowship
732 (AD), a University of Glasgow Lord Kelvin Adam Smith Scholarship (RI), and funds from the University
733 of Glasgow Wellcome Trust Institutional Strategic Support award (RI and AD).

Bibliography

1. Cabreiro, F. *et al.* Metformin Retards Aging in C. elegans by Altering Microbial Folate and Methionine Metabolism. *Cell* **153**, 228–239 (2013).

2. Pryor, R. *et al.* Host-Microbe-Drug-Nutrient Screen Identifies Bacterial Effectors of Metformin Therapy. *Cell* (2019) doi:10.1016/j.cell.2019.08.003.

3. Houthoofd, K. *et al.* Axenic growth up-regulates mass-specific metabolic rate, stress resistance, and extends life span in Caenorhabditis elegans. *Experimental gerontology* **37**, 1371–8 (2002).

4. Sannino, D. R., Dobson, A. J., Edwards, K., Angert, E. R. & Buchon, N. The Drosophila melanogaster Gut Microbiota Provisions Thiamine to Its Host. *mBio* **9**, (2018).

5. Brummel, T., Ching, A., Seroude, L., Simon, A. F. & Benzer, S. Drosophila lifespan enhancement by exogenous bacteria. *Proceedings of the National Academy of Sciences of the United States of America* **101**, 12974–12979 (2004).

6. Matthews, M. K. *et al.* Genetic Influences of the Microbiota on the Life Span of Drosophila melanogaster. *Appl Environ Microb* **86**, (2020).

7. Obata, F., Fons, C. O. & Gould, A. P. Early-life exposure to low-dose oxidants can increase longevity via microbiome remodelling in Drosophila. *Nat. Commun.* **9**, 975 (2018).

8. Smith, P. *et al.* Regulation of life span by the gut microbiota in the short-lived African turquoise killifish. *eLife* **6**, (2017).

9. Valenzano, D. *et al.* The African Turquoise Killifish Genome Provides Insights into Evolution and Genetic Architecture of Lifespan. *Cell* **163**, 1539–1554 (2015).

10. Snyder, D., Pollard, M., Wostmann, B. & Luckert, P. Life span, morphology, and pathology of diet-restricted germ-free and conventional Lobund-Wistar rats. *Journal of gerontology* **45**, B52-8 (1990).

11. Gordon, H. A., Bruckner-Kardoss, E. & Wostmann, B. S. Aging in germ-free mice: life tables and lesions observed at natural death. *Journal of gerontology* **21**, 380–7 (1966).

12. Tazume, S. *et al.* Effects of germfree status and food restriction on longevity and growth of mice. *Jikken dobutsu. Experimental animals* **40**, 517–22 (1991).

13. OToole, P. & Jeffery, I. Gut microbiota and aging. *Science* **350**, 1214–1215 (2015).

14. Johansen, J. *et al.* Centenarians have a diverse gut virome with the potential to modulate metabolism and promote healthy lifespan. *Nat. Microbiol.* **8**, 1064–1078 (2023).

15. Liu, X. *et al.* Mendelian randomization analyses reveal causal relationships between the human microbiome and longevity. *Sci. Rep.* **13**, 5127 (2023).

16. Gagnon, E. *et al.* Impact of the gut microbiota and associated metabolites on cardiometabolic traits, chronic diseases and human longevity: a Mendelian randomization study. *J. Transl. Med.* **21**, 60 (2023).

17. Williams, G. C. Pleiotropy, natural selection, and the evolution of senescence. . *Evolution* **11**, (1957).

771 18. Schwarzer, M. *et al.* Lactobacillus plantarum strain maintains growth of infant mice during chronic
772 undernutrition. *Science (New York, N.Y.)* **351**, 854–7 (2016).

773 19. Storelli, G. *et al.* Lactobacillus plantarum promotes Drosophila systemic growth by modulating
774 hormonal signals through TOR-dependent nutrient sensing. *Cell metabolism* **14**, 403–14 (2011).

775 20. Wong, A., Dobson, A. J. & Douglas, A. E. Gut microbiota dictates the metabolic response of
776 Drosophila to diet. *The Journal of Experimental Biology* **217**, 1894–1901 (2014).

777 21. Liu, X. *et al.* Microbes affect gut epithelial cell composition through immune-dependent regulation
778 of intestinal stem cell differentiation. *Cell Reports* **38**, 110572 (2022).

779 22. Broderick, N. A., Buchon, N. & Lemaitre, B. Microbiota-induced changes in drosophila
780 melanogaster host gene expression and gut morphology. *mBio* **5**, e01117-14 (2014).

781 23. Bost, A. *et al.* How gut transcriptional function of Drosophila melanogaster varies with the
782 presence and composition of the gut microbiota. *Mol Ecol* **27**, 1848–1859 (2018).

783 24. Rewitz, K. *et al.* Protein-responsive gut hormone Tachykinin directs food choice and impacts
784 lifespan in Drosophila. (2024) doi:10.21203/rs.3.rs-3837414/v1.

785 25. Song, W., Veenstra, J. A. & Perrimon, N. Control of Lipid Metabolism by Tachykinin in Drosophila.
786 *Cell Reports* (2014) doi:10.1016/j.celrep.2014.08.060.

787 26. Wong, A. C.-N., Dobson, A. J. & Douglas, A. E. Gut microbiota dictates the metabolic response of
788 Drosophila to diet. *J Exp Biology* **217**, 1894–1901 (2014).

789 27. Dobson, A. J. *et al.* Host genetic determinants of microbiota-dependent nutrition revealed by
790 genome-wide analysis of Drosophila melanogaster. *Nature communications* **6**, 6312 (2015).

791 28. Moullan, N. *et al.* Tetracyclines Disturb Mitochondrial Function across Eukaryotic Models: A Call
792 for Caution in Biomedical Research. *Cell Rep.* **10**, 1681–1691 (2015).

793 29. Chatzispyrou, I. A., Held, N. M., Mouchiroud, L., Auwerx, J. & Houtkooper, R. H. Tetracycline
794 Antibiotics Impair Mitochondrial Function and Its Experimental Use Confounds Research. *Cancer*
795 *Res.* **75**, 4446–4449 (2015).

796 30. Ronayne, C. T. *et al.* Tetracyclines activate mitoribosome quality control and reduce ER stress to
797 promote cell survival. *EMBO Rep.* **24**, e57228 (2023).

798 31. Nässel, D. R. What Drosophila can tell us about state-dependent peptidergic signaling in insects.
799 *Insect Biochem. Mol. Biol.* 104275 (2025) doi:10.1016/j.ibmb.2025.104275.

800 32. Partridge, L., Gems, D. & Withers, D. J. Sex and Death: What Is the Connection? *Cell* **120**,
801 (2005).

802 33. Flatt, T. Ageing: Diet and longevity in the balance. *Nature* **462**, 989–990 (2009).

803 34. Good, T. & Tatar, M. Age-specific mortality and reproduction respond to adult dietary restriction in
804 Drosophila melanogaster. (2001).

805 35. Grandison, R. C., Piper, M. D. & Partridge, L. Amino-acid imbalance explains extension of lifespan
806 by dietary restriction in Drosophila. *Nature* **462**, 1061–1064 (2009).

807 36. Mair, W., Piper, M. D. & Partridge, L. Calories Do Not Explain Extension of Life Span by Dietary
808 Restriction in Drosophila. *PLoS Biology* **3**, e223 (2005).

809 37. Turnbaugh, P. J. *et al.* An obesity-associated gut microbiome with increased capacity for energy
810 harvest. *Nature* **444**, 1027 (2006).

811 38. Vijay-Kumar, M. *et al.* Metabolic Syndrome and Altered Gut Microbiota in Mice Lacking Toll-Like
812 Receptor 5. *Science* **328**, 228–231 (2010).

813 39. Wong, A. C.-N., Chaston, J. M. & Douglas, A. E. The inconstant gut microbiota of Drosophila
814 species revealed by 16S rRNA gene analysis. *ISME J.* **7**, 1922–1932 (2013).

815 40. Wang, Y. & Staubach, F. Individual variation of natural D.melanogaster-associated bacterial
816 communities. *FEMS Microbiol. Lett.* **365**, fny017 (2018).

817 41. Brown, J. J. *et al.* Microbiome structure of a wild Drosophila community along tropical elevational
818 gradients and comparison to laboratory lines. *bioRxiv* 2021.07.28.454263 (2023)
819 doi:10.1101/2021.07.28.454263.

820 42. Staubach, F., Baines, J. F., Kuenzel, S., Bik, E. M. & Petrov, D. A. Host species and
821 environmental effects on bacterial communities associated with Drosophila in the laboratory and in
822 the natural environment. *arXiv* (2012) doi:10.48550/arxiv.1211.3367.

823 43. Chandler, J. A., Lang, J. M., Bhatnagar, S., Eisen, J. A. & Kopp, A. Bacterial Communities of
824 Diverse Drosophila Species: Ecological Context of a Host–Microbe Model System. *PLoS Genet.* **7**,
825 e1002272 (2011).

826 44. Newell, P. D. *et al.* In vivo function and comparative genomic analyses of the Drosophila gut
827 microbiota identify candidate symbiosis factors. *Front. Microbiol.* **5**, 576 (2014).

828 45. Newell, P. D. & Douglas, A. E. Interspecies Interactions Determine the Impact of the Gut
829 Microbiota on Nutrient Allocation in Drosophila melanogaster. *Appl. Environ. Microbiol.* **80**, 788–796
830 (2014).

831 46. Leader, D. P., Krause, S. A., Pandit, A., Davies, S. A. & Dow, J. A. T. FlyAtlas 2: a new version of
832 the Drosophila melanogaster expression atlas with RNA-Seq, miRNA-Seq and sex-specific data.
833 *Nucleic Acids Res.* **46**, D809–D815 (2018).

834 47. Jugder, B.-E., Kamareddine, L. & Watnick, P. I. Microbiota-derived acetate activates intestinal
835 innate immunity via the Tip60 histone acetyltransferase complex. *Immunity* **54**, 1683-1697.e3 (2021).

836 48. Scopelliti, A. *et al.* Local Control of Intestinal Stem Cell Homeostasis by Enteroendocrine Cells in
837 the Adult Drosophila Midgut. *Current Biology* **24**, (2014).

838 49. Lin, H.-H. *et al.* A nutrient-specific gut hormone arbitrates between courtship and feeding. *Nature*
839 **602**, 632–638 (2022).

840 50. Medina, A. B. *et al.* Neuroendocrine Control of Intestinal Regeneration Through the Vascular
841 Niche in Drosophila. *bioRxiv* 2024.09.10.612352 (2024) doi:10.1101/2024.09.10.612352.

842 51. Malita, A. *et al.* A gut-derived hormone suppresses sugar appetite and regulates food choice in
843 Drosophila. *Nat. Metab.* **4**, 1532–1550 (2022).

844 52. Kubrak, O. *et al.* The gut hormone Allatostatin C/Somatostatin regulates food intake and
845 metabolic homeostasis under nutrient stress. *Nat Commun* **13**, 692 (2022).

846 53. Nässel, D. R., Zandawala, M., Kawada, T. & Satake, H. Tachykinins: Neuropeptides That Are
847 Ancient, Diverse, Widespread and Functionally Pleiotropic. *Front. Neurosci.* **13**, 1262 (2019).

848 54. Rera, M., Clark, R. & Walker, D. Intestinal barrier dysfunction links metabolic and inflammatory
849 markers of aging to death in Drosophila. *Proceedings of the National Academy of Sciences* **109**,
850 (2012).

851 55. Zane, F. *et al.* Smurfness-based two-phase model of ageing helps deconvolve the ageing
852 transcriptional signature. *Aging Cell* **22**, e13946 (2023).

853 56. Clark, R. I. *et al.* Distinct Shifts in Microbiota Composition during Drosophila Aging Impair
854 Intestinal Function and Drive Mortality. *Cell reports* **12**, 1656–67 (2015).

855 57. Regan, J. C. *et al.* Sex difference in pathology of the ageing gut mediates the greater response of
856 female lifespan to dietary restriction. *eLife* **5**, e10956 (2016).

857 58. Clancy, D. J. *et al.* Extension of Life-Span by Loss of CHICO, a Drosophila Insulin Receptor
858 Substrate Protein. *Science* **292**, 104–106 (2001).

859 59. Kenyon, C., Chang, J., Gensch, E., Rudner, A. & Tabtiang, R. A C. elegans mutant that lives twice
860 as long as wild type. *Nature* **366**, 461 (1993).

861 60. Selman, C. *et al.* Evidence for lifespan extension and delayed age–related biomarkers in insulin
862 receptor substrate 1 null mice. *Faseb J* **22**, 807–818 (2008).

863 61. Slagboom, P. E., Berg, N. van den & Deelen, J. Phenome and genome based studies into human
864 ageing and longevity: An overview. *Biochimica Et Biophysica Acta Mol Basis Dis* **1864**, 2742–2751
865 (2017).

866 62. Shin, S. *et al. Drosophila* Microbiome Modulates Host Developmental and Metabolic Homeostasis
867 via Insulin Signaling. *Science* **334**, 670–674 (2011).

868 63. Birse, R. T., Söderberg, J. A., Luo, J., Winther, Å. M. & Nässel, D. R. Regulation of insulin-
869 producing cells in the adult Drosophila brain via the tachykinin peptide receptor DTKR. *The Journal of*
870 *Experimental Biology* **214**, 4201–4208 (2011).

871 64. Broughton, S. J. *et al.* Longer lifespan, altered metabolism, and stress resistance in Drosophila
872 from ablation of cells making insulin-like ligands. *Proceedings of the National Academy of Sciences of*
873 *the United States of America* **102**, 3105–3110 (2005).

874 65. Alic, N. *et al.* Cell-nonautonomous effects of dFOXO/DAF-16 in aging. *Cell reports* **6**, (2014).

875 66. Slack, C., Giannakou, M. E., Foley, A., Goss, M. & Partridge, L. dFOXO-independent effects of
876 reduced insulin-like signaling in Drosophila. *Aging Cell* **10**, 735–748 (2011).

877 67. Slack, C. *et al.* The Ras-Erk-ETS-Signaling Pathway Is a Drug Target for Longevity. *Cell* **162**, 72–
878 83 (2015).

879 68. Musselman, L. P., Kühnlein, R. P., Suarez, R. K. & Hoppeler, H. H. Drosophila as a model to
880 study obesity and metabolic disease. *J. Exp. Biol.* **221**, jeb163881 (2018).

881 69. Gäde, G. & Marco, H. G. The Adipokinetic Peptides of Hemiptera: Structure, Function, and
882 Evolutionary Trends. *Front. Insect Sci.* **2**, 891615 (2022).

883 70. Toprak, U., Hegedus, D., Doğan, C. & Güney, G. A journey into the world of insect lipid
884 metabolism. *Arch. Insect Biochem. Physiol.* **104**, e21682 (2020).

885 71. Seidel, J. & Valenzano, D. The role of the gut microbiome during host ageing. *F1000Research* **7**,
886 F1000 Faculty Rev-1086 (2018).

887 72. Cui, R. *et al.* Relaxed Selection Limits Lifespan by Increasing Mutation Load. *Cell* (2019)
888 doi:10.1016/j.cell.2019.06.004.

889 73. Qansuwa, E. M. *et al.* Handbook of Neurodegenerative Disorders. 17–41 (2024) doi:10.1007/978-
890 981-99-7557-0_2.

891 74. Boehme, M., Guzzetta, K. E., Wasén, C. & Cox, L. M. The gut microbiota is an emerging target for
892 improving brain health during ageing. *Gut Microbiome* **4**, e2 (2022).

893 75. Dinan, T. G. & Cryan, J. F. Gut instincts: microbiota as a key regulator of brain development,
894 ageing and neurodegeneration. *J. Physiol.* **595**, 489–503 (2017).

895 76. Regan, J. C. & Partridge, L. Gender and longevity: Why do men die earlier than women?
896 Comparative and experimental evidence. *Best Pr. Res. Clin. Endocrinol. Metab.* **27**, 467–479 (2013).

897 77. Buchon, N., Broderick, N. A., Chakrabarti, S. & Lemaitre, B. Invasive and indigenous microbiota
898 impact intestinal stem cell activity through multiple pathways in Drosophila. *Genes & development* **23**,
899 2333–44 (2009).

900 78. Watnick, P. I. & Jugder, B.-E. Microbial Control of Intestinal Homeostasis via Enteroendocrine Cell
901 Innate Immune Signaling. *Trends Microbiol.* **28**, 141–149 (2020).

902 79. Kim, B. *et al.* Response of the microbiome–gut–brain axis in Drosophila to amino acid deficit.
903 *Nature* **593**, 570–574 (2021).

904 80. Guo, X. *et al.* The Cellular Diversity and Transcription Factor Code of Drosophila Enteroendocrine
905 Cells. *Cell Reports* **29**, 4172-4185.e5 (2019).

906 81. Ahrentløv, N. *et al.* Protein-responsive gut hormone tachykinin directs food choice and impacts
907 lifespan. *Nat. Metab.* **7**, 1223–1245 (2025).

908 82. Shin, S. C. *et al. Drosophila* Microbiome Modulates Host Developmental and Metabolic
909 Homeostasis via Insulin Signaling. *Science* **334**, 670–674 (2011).

910 83. Huang, J.-H. & Douglas, A. E. Consumption of dietary sugar by gut bacteria determines
911 Drosophila lipid content. *Biology Letters* **11**, 20150469 (2015).

912 84. Dobson, A. J., Chaston, J. M. & Douglas, A. E. The Drosophila transcriptional network is
913 structured by microbiota. *BMC genomics* **17**, 975 (2016).

914 85. Clark, R. I. & Walker, D. W. Role of gut microbiota in aging-related health decline: insights from
915 invertebrate models. *Cellular and Molecular Life Sciences* (2017) doi:10.1007/s00018-017-2671-1.

916 86. Bjedov, I., Toivonen, J., Kerr, F., Slack, C. & Jacobson, J. Mechanisms of life span extension by
917 rapamycin in the fruit fly Drosophila melanogaster. (2010).

918 87. Zhang, A. *et al.* Characterization of Effects of mTOR Inhibitors on Aging in Caenorhabditis
919 elegans. *J. Gerontol., Ser. A: Biol. Sci. Méd. Sci.* **79**, glae196 (2024).

920 88. Miller, R. A. *et al.* Rapamycin-mediated lifespan increase in mice is dose and sex dependent and
921 metabolically distinct from dietary restriction. *Aging Cell* **13**, 468–477 (2014).

922 89. Wilkinson, J. E. *et al.* Rapamycin slows aging in mice: Rapamycin slows aging in mice. *Aging Cell*
923 **11**, 675–682 (2012).

924 90. Harrison, D. E. *et al.* Rapamycin fed late in life extends lifespan in genetically heterogeneous
925 mice. *Nature* **460**, 392–395 (2009).

926 91. Sass, F. *et al.* NK2R control of energy expenditure and feeding to treat metabolic diseases.
927 *Nature* **635**, 987–1000 (2024).

928 92. Bass, T. M. *et al.* Optimization of Dietary Restriction Protocols in Drosophila. *Journals*
929 *Gerontology Ser* **62**, 1071–1081 (2007).

930 93. Sannino, D. R. & Dobson, A. J. Acetobacter pomorum in the Drosophila gut microbiota buffers
931 against host metabolic impacts of dietary preservative formula and batch variation in dietary yeast.
932 *Appl. Environ. Microbiol.* **89**, e00165-23 (2023).

933 94. Fossati, P. & Prencipe, L. Serum triglycerides determined colorimetrically with an enzyme that
934 produces hydrogen peroxide. *Clin Chem* **28**, 2077–2080 (1982).

935 95. Team, R. C. R: A language and environment for statistical computing. (2024).

936 96. Patro, R., Duggal, G., Love, M. I., Irizarry, R. A. & Kingsford, C. Salmon provides fast and bias-
937 aware quantification of transcript expression. *Nat. Methods* **14**, 417–419 (2017).

938

939

940 ## Supplementary figure legends

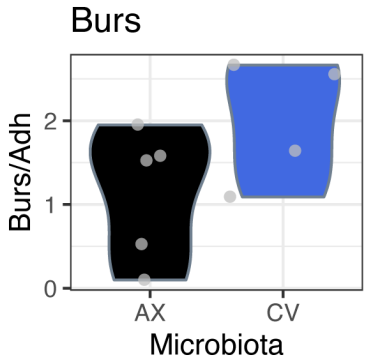

941

942 **Figure S1. Microbiota do not alter *Burs* expression.** Expression was quantified by RT-qPCR (using
943 cDNA generated from midgut to complement RNA-seq data) because transcripts were not quantified
944 from RNA-seq data (Figure 1). No significant difference in expression was detected (t=-1.65, p=0.15).

945

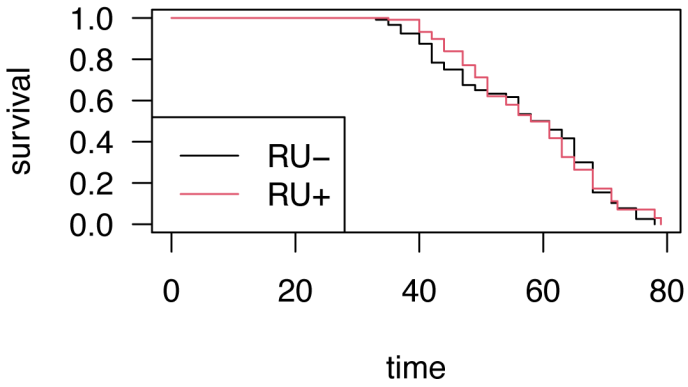

946

947 **Figure S2. Lifespan extension by feeding RU to CR *DaGS;UAS-Tk^{RNAi}* flies is not attributable to**
948 **off-target effects of RU or GeneSwitch activation.** Kaplan-Meier plot shows impact of feeding RU to
949 *DaGS/+* flies reared with complete microbiota. No effect of RU was detected (Cox Proportional Hazards
950 p=0.5).

951

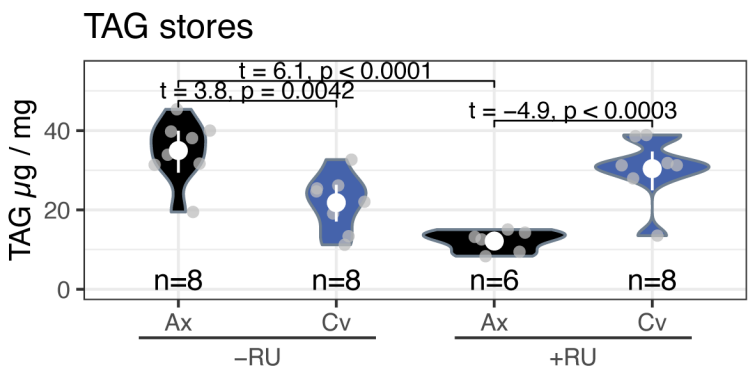

952

953 **Figure S3. Interactive effect of *TkRNAi* and microbiota on TAG levels confirmed with**
954 **independent RNAi construct.** The experiment presented in Figure 2E (which used construct
955 V330743) was repeated with an independent construct (V103668). The same result was replicated.

956 Violin plots show density of datapoints, mean±CI95 given in white. ANOVA (Type 3 tests),
957 microbiota:RU $F_{1,26}$=37.86, p=1.66e-06. Statistics on brackets are from *post-hoc* EMM analyses of
958 linear model, when significant differences were detected.
959

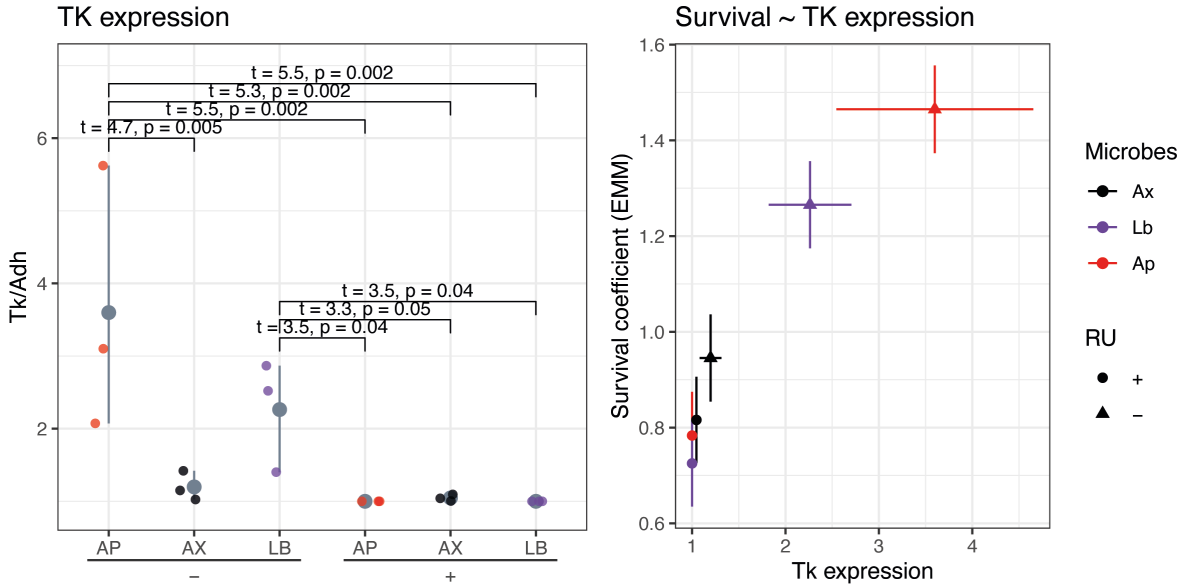

960
961 **Figure S4. Modulation of *Tk* expression by microbiota correlates lifespan outcome. A.** RT-qPCR
962 indicates elevated *Tk* expression in *Ap*-flies above levels in axenics and *Lb*-flies, and above levels in
963 all conditions expressing Tk^{RNAi}. Expression in *Lb*-flies was significantly greater than in conditions
964 expressing Tk^{RNAi}, but not significantly greater than axenics without Tk^{RNAi} expression. Statistics on
965 brackets are from *post-hoc* EMM analyses of linear model, when significant differences were detected.
966 **B.** *Tk* expression differences across microbiota and Tk^{RNAi} conditions correlate lifespan differences. *Tk*
967 expression from panel A is plotting against survival coefficients of lifespan experiment shown in Figure
968 3c-d.
969

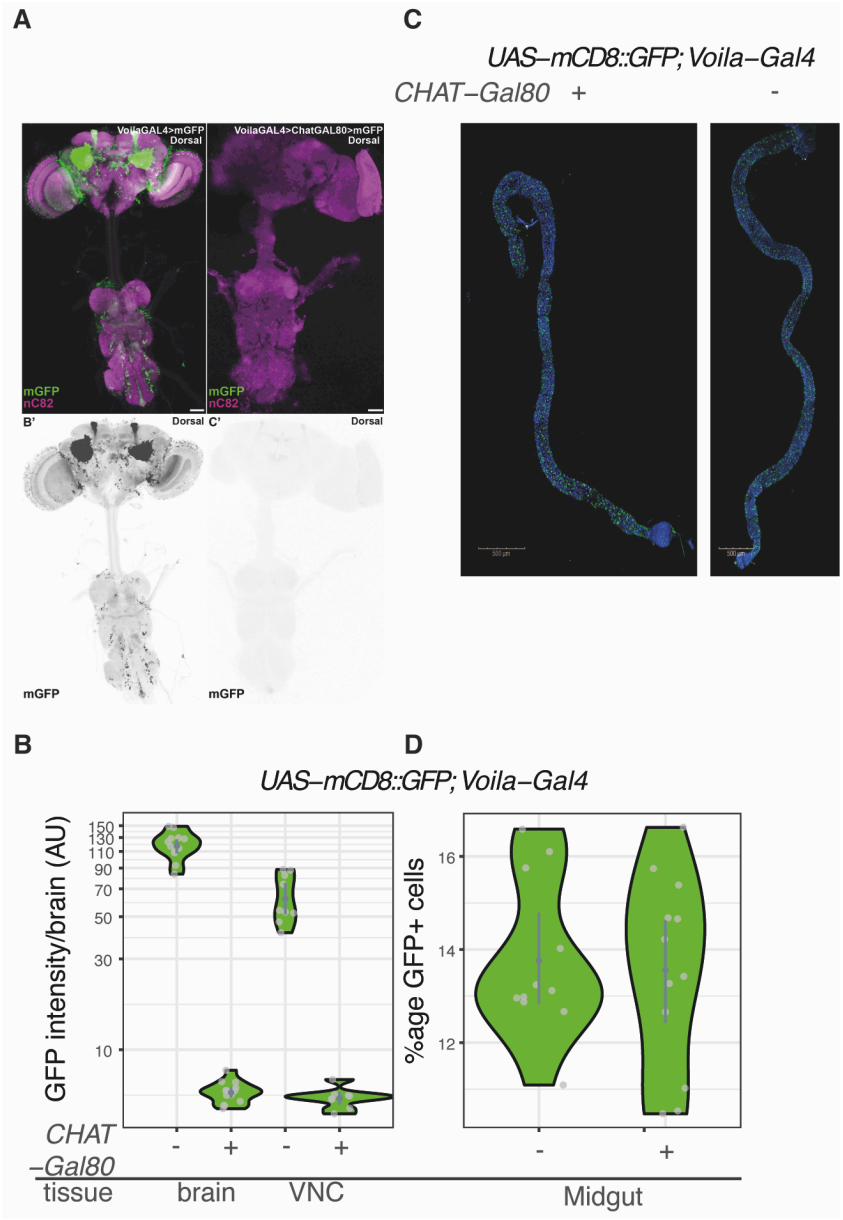

Figure S5. Intersectional Gal80 strategy to direct Gal4 activity to enteroendocrine cells, sparing CNS. As per Medina et al [50], we tested the capacity of Gal80 expressed under control of the *ChAT* promoter to repress Gal4 expressed under control of the *Voila* promoter, assayed by expression of *UAS-mCD8::GFP.* **A.** Representative confocal micrographs of CNS, and **B.** Quantification of Voila>GFP intensity in brain and CNS, in presence/absence of *Voila Gal80*. **C.** Representative confocal micrographs of midgut (region 4). **D.** Number of GFP+ cells/ROI in presence/absence of *Voila Gal80.*

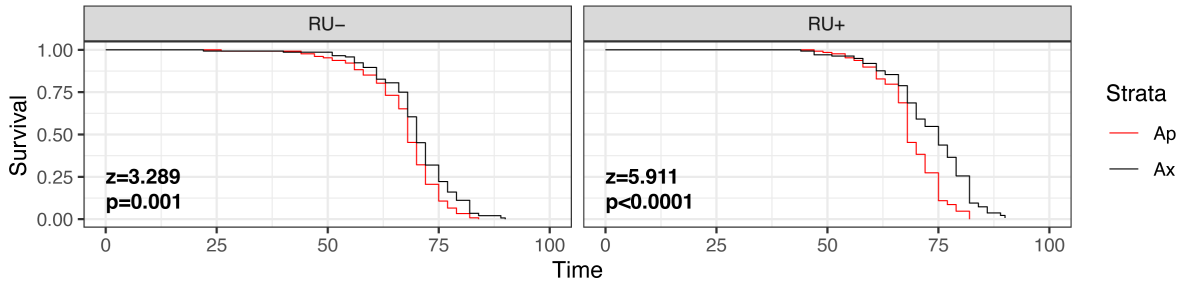

Figure S6. *TkR99D*^{RNAi} induction in enterocytes does not block impact of *A. pomorum* on lifespan. Expression was driven with *Mex1-GeneSwitch*. Statistics in panel from Cox proportional hazards model, reporting post-hoc (EMM) analysis for effect of RU per microbiota condition.

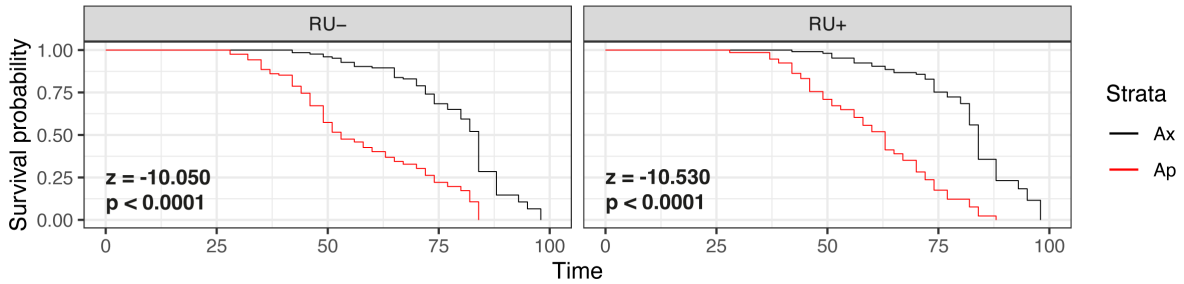

Figure S7. *AkhR*^{RNAi} induction in fat body (and gut) does not block impact of *A. pomorum* on lifespan. Expression was driven with *S106-GeneSwitch*. Statistics in panel from Cox proportional hazards model, reporting post-hoc (EMM) analysis for effect of RU per microbiota condition.